Manuscript Details

Manuscript number QUATINT_2016_949

Title Sediment trapping in deltas of small mountainous rivers of southwestern Taiwan and its influence on East China Sea sedimentation

Article type Full Length Article

Abstract

Taiwan's setting of high mountains, steep gradients, frequent earthquakes, erodible lithology, and heavy rainfall represents an ideal site to focus on sedimentary processes of the deltas of small mountainous rivers (SMRs). Several SMRs in southwestern Taiwan have deposited a thick sedimentary succession in the composite Southwest Taiwan Delta (SWTD) since the middle Holocene. Evidence from the SWTD can help to determine its trapping efficiency and assess the role of SMRs in sediment transport to the sea. We used historical nautical charts, bathymetric data, satellite radar data, and 14C dates to calculate the sediment volume of the SWTD on millennial and decadal scales. The 14C dates of core samples indicate deposition of thick deltaic sediment in subsiding areas since the time of the maximum flooding surface about 7 cal ka BP. The paleo-shoreline changes of the SWTD suggest a steady westward progradation since 7 cal ka BP. In contrast, the nautical charts suggest minor volume reduction of the offshore part of the SWTD, with a deepening trend and retreating shorelines, during the last seven decades. The results show that at least 201.72 ± 13.90 km3 (~3.23 × 105 Mt) of sediment has been trapped in the SWTD since 7 cal ka BP, and that the delta has shifted to a destructive phase during the past seven decades as human influences such as construction of reservoirs, dams, and weirs in the hills have reduced the sediment supply. The birth of the Taiwan Warm Current and following continuous sediment supply from the western rivers of Taiwan to the East China Sea since ~7.3 cal ka BP have played a crucial role in the sedimentation of the East China Sea, particularly in the Okinawa Trough, and the Japan Sea through the Tsushima Warm Current.

Keywords small-mountainous-river deltas; sediment trapping; Taiwan Warm Current; East China Sea; sediment provenance; Kuroshio.

Corresponding Author Kan-Hsi Hsiung

Corresponding Author's Institution Japan Agency for Marine-Earth Science and Technology

Order of Authors Kan-Hsi Hsiung, SAITO YOSHIKI

Suggested reviewers Paul Liu, John Milliman, Kazuaki Hori, Chih-Chieh Su

Sediment trapping in deltas of small mountainous rivers of southwestern Taiwan and its influence on East China Sea sedimentation

Kan-Hsi Hsiung[a,b *], Yoshiki Saito[b,c*]

[a]Research and Development Center for Ocean Drilling Science, Yokohama Institute for Earth Sciences, JAMSTEC, 3173-25 Showa-machi, Kanazawa-ku, Yokohama, Kanagawa 236-0001, Japan

[b]Geological Survey of Japan, AIST, Central 7, 1-1-1 Higashi, Tsukuba, Ibaraki 305-8567, Japan

[c]ReCCLE, Shimane University, 1060 Nishikawatsu-cho, Matsue, Shimane 690-8504, Japan

* Corresponding author: hsiung@jamstec.go.jp (K.H. Hsiung); ysaito@soc.shimane-u.ac.jp (Y. Saito)

Abstract

Taiwan's setting of high mountains, steep gradients, frequent earthquakes, erodible lithology, and heavy rainfall represents an ideal site to focus on sedimentary processes of the deltas of small mountainous rivers (SMRs). Several SMRs in southwestern Taiwan have deposited a thick sedimentary succession in the composite Southwest Taiwan Delta (SWTD) since the middle Holocene. Evidence from the SWTD can help to determine its trapping efficiency and assess the role of SMRs in sediment transport to the sea. We used historical nautical charts, bathymetric data, satellite radar data, and ^{14}C dates to calculate the sediment volume of the SWTD on millennial and decadal scales. The ^{14}C dates of core samples indicate deposition of thick deltaic sediment in subsiding areas since the time of the maximum flooding surface about 7 cal ka BP. The paleo-shoreline changes of the SWTD suggest a steady westward progradation since 7 cal ka BP. In contrast, the nautical charts suggest minor volume reduction of the offshore part of the SWTD, with a deepening trend and retreating shorelines, during the last seven decades. The results show that at least 201.72 ± 13.90 km^3 (~3.23 × 10^5 Mt) of sediment has been trapped in the SWTD since 7 cal ka BP, and that the delta has shifted to a destructive phase during the past seven decades as human influences such as construction of reservoirs, dams, and weirs in the hills have reduced the sediment supply. The birth of the Taiwan Warm Current and following continuous sediment supply from the western rivers of Taiwan to the East China Sea since ~7.3 cal ka BP have played a crucial role in the sedimentation of the East China Sea, particularly in the Okinawa Trough, and the Japan Sea through the Tsushima Warm Current.

Keywords: small-mountainous-river deltas; sediment trapping; Taiwan Warm Current; East China Sea; sediment provenance; the Kuroshio.

1. Introduction

Deltas form in coastal environments where river-borne sediment builds sedimentary bodies that extend by aggradation into receiving basins. Wright (1977) defined deltas as "coastal accumulations, both subaqueous and subaerial, of river-derived sediments adjacent to, or in close proximity to, the source stream," and Elliott (1978) defined them as "discrete shoreline protuberances formed where rivers enter oceans, semi-enclosed seas, lakes or barrier-sheltered lagoons and supply sediment more rapidly than it can be redistributed by indigenous basinal processes." Modern deltas are widely variable in terms of scale, processes and the nature of the sediment deposits. Deltas are commonly classified as dominated by rivers, waves or tides (Galloway, 1975) and are also classified using grain-size factors (Orton and Reading, 1993).

Most modern deltas have been built since 7.5–8.0 cal ka BP, following the decrease of Holocene sea-level rise (Stanley and Warne, 1994; Olariu, 2014). High-resolution studies of deltas and sea-level changes have revealed that delta initiation occurred after a rapid rise of sea level during 9.0–8.2 cal ka BP, and the timing of delta initiation depended on the sediment supply between 8.2 and 6.5 cal ka BP (e.g., Tamura et al., 2009; Hijma and Cohen, 2010; Smith et al., 2011; Li et al., 2012b; Wang et al., 2013; Song et al., 2013; Tjallingii et al., 2014). Large deltas are major sinks of terrestrial sediment in coastal areas (e.g., Bianchi and Allison, 2009), and deltas usually have higher accumulation rates than other marine environments (Syvitski, 2003).

Rivers in Asia and Oceania deliver huge amounts of sediment, amounting to ~70% of the global discharge of suspended sediment (Milliman and Farnsworth, 2011), with large rivers on the Asian continent and small rivers on islands contributing roughly equal portions. Many recent studies of the Holocene deltas of large Asian rivers have focused on delta evolution, sediment facies, paleo-environments, and sediment flux and fate (e.g., Woodroffe et al., 2006; Liu et al., 2009; Woodroffe and Saito, 2011; Wang et al., 2011; Wilson and Goodbred, 2015). The East Indies (Oceania) constitutes one of the largest regional sources of sediment to the global ocean (Milliman et al., 1999). The Fly River delta of New Guinea, one of the largest deltas in Oceania in terms of sediment discharge, is comparable to large river deltas and has been well characterized (Dalrymple et al., 2003). However, deltas associated with small mountainous rivers (SMRs) are not well studied. In this study we examined the large composite Holocene delta of southwestern Taiwan, which is a good example of SMR deltas, to characterize its sediment trapping and delta evolution at millennial and decadal time scales.

Taiwan's natural setting of high mountains, steep gradients, frequent earthquakes, erodible lithology, and heavy rainfall makes it a natural laboratory for studying the fate of sediment transport by SMRs. For example, events including typhoons, earthquakes and extreme rainfall trigger erosion and weathering of rocks that in turn promote sediment output. Landslides induced by earthquakes mobilize large volumes of sediment that is susceptible to erosion during typhoon and monsoon seasons (Dadson et al., 2004; Milliman et al., 2007). Consequently, the mountain ranges of Taiwan deliver very large quantities of sediment to the coast. Estimates of the average amounts of sediment delivered to the ocean by Taiwanese rivers include one of 384 Mt/y during 1970–1998 (Dadson et al., 2003) and another of 180 Mt/y of sediment between the 1980s and 2005, with a range of 16 to 440 Mt/y (Kao and Milliman, 2008). These estimates rival the sediment discharges of the Mekong (160 Mt/y) and Red (130 Mt/y) rivers, as well as that of the Yangtze River (~150 Mt/y) after completion of the Three Gorges Dam and the Yellow River (~150 Mt) after completion of the Xiaolangdi Dam (Wang et al., 2011). This study focused on sediment trapping in the Chianan Plain, a wide compound delta plain (Fig. 1) in southwestern Taiwan, and the influence of sediment from this area on sedimentation in the East China Sea.

2. Geological background

The Taiwan orogen, resulting from oblique collision between the Luzon Arc and the Eurasian continent (Fig. 1), manifests as a mountain belt reaching elevations of 4 km (Bowin et al., 1978; Ho, 1988; Teng, 1990). The denudation rate of the Central Range of Taiwan has averaged at least 1.4 $g/cm^2/y$ since the Pliocene (Li, 1976). Furthermore, the erosion rate ranges from 3 to 6 mm/y for an average annual sediment yield of 500 Mt/y, and much of the bedload in Taiwanese rivers is trapped in floodplains before reaching the sea (Dadson et al., 2003). Under precipitation totals of ~2500 mm/y, the SMRs of Taiwan are strongly affected by periodic floods, typhoons, and earthquakes (Dadson et al., 2003; Kao and Milliman, 2008). Sediment transport in SMR catchments is substantially influenced by landslide debris produced by hillslope mass wasting (Hovius et al., 2000). The SMRs of western Taiwan run perpendicular to the strike of the Taiwan orogen in short, straight routes across low-gradient deltaic plains (Fig. 1) and thus tend to discharge larger percentages of their sediment loads directly to the sea than do larger rivers. However, eight of these SMRs (the Choshui, Peikang, Potzu, Pachang, Chishui, Tsengwen, Yenshui, and Erhjen rivers; see Table 1) have collectively built up a compound delta, called here the Southwest Taiwan Delta (SWTD), in the western and southwestern coastal plains (Fig. 1). The Choshui and Tsengwen rivers are major rivers longer than 100 km whereas the others are shorter (Table 1). The total drainage basin area of the eight SMRs is 6953 km^2. The SWTD consists of a subaerial portion with an area of about 5000 km^2 and a subaqueous portion amounting to 2000 km^2 (Fig. 1).

The SWTD owes its elongated form partly to its multiple sediment supplies and partly to the tectonic and structural restrictions posed by the Chukou and Chelungpu thrust faults to the east, the Changhua-Pakuashan anticline to the north and the Laonung fault to the south (Shyu et al., 2005). To the west, the Taiwan Strait is a seaway about 140 km wide with a mean water depth around 60 m, connecting the East China Sea and the South China Sea (Fig. 2). Features on the floor of the Taiwan Strait, including the west and east Changyun sand ridges, Penghu Channel and Taiwan Bank, are products of the modern tidal current system (Chern and Wang, 2000; Yu and Huang, 2003; Liao and Yu, 2005). The south part of the Taiwan Strait is relatively shallow by the Taiwan Bank and Penghu Islands. The east Changyun sand ridge lies directly off the northern part of the subaqueous delta. To its south, the funnel-shaped Penghu Channel runs N–S between the Penghu Islands and southwestern Taiwan (Liao and Yu, 2005). The northern part of the subaqueous delta extends to about 40 m depth in front of the east Changyun sand ridge, and the southern part extends down to about 100 m east of the Penghu Channel (Fig. 2). The southwestern part of the delta near Tainan includes a series of lagoons and lakes along the current shoreline (Yang and Su, 2001). The average tidal current in the Taiwan Strait is 0.46 m/s with a range of 0.2–0.8 m/s, and the average mean current is about 0.40 m/s (Wang et al., 2003).

The sea level in the Taiwan Strait west of Taiwan has been relatively stable since 7 cal ka BP (Chen and Liu, 1996, 2000). In southwestern Taiwan, the first major transgression began prior to ~8.5 cal ka BP (7.68 ^{14}C ka BP) and the maximum transgression occurred about ~6.8 cal ka BP (6.0 ^{14}C ka BP) (Taira, 1975). For example, Figure 3 shows that the chronology in core TN-SF was determined from six ^{14}C ages. The interval from 20 to 85 m core depth was characterized by marine facies, and the maximum flooding surface was identified at 46.3 m with an age of 7 cal ka BP. The Holocene sediments of the SWTD consist mainly of sand, gravel, and some clay plus substantial soil carbonate (Lin, 1969; Ho, 1988; Dadson et al., 2003). The Holocene and late Pleistocene stratigraphy of the Choshui and Tsengwen river deltas has been derived from core drilling in the Choshui Delta, which yielded numerous ^{14}C dates (Chen and Liu, 2003; Chen et al., 2010) that are listed in Table 2.

3. Data and methods

3.1 Paleo-bathymetry evaluation on a decadal timescale

We compiled historical charts made by organizations in Taiwan and Japan to map the shorelines and bathymetry off western Taiwan in 1930 (Fig. 4a) and 2002 (Fig. 4b). We also used the present-day bathymetry (about 2010) to evaluate bathymetric changes. Decadal-scale coastal changes can be discerned during the intervals 1930–2002 and 2002–present (Fig. 4c). We calculated sediment volume changes from these charts with respect to the modern shoreline, using MATLAB functions in the Statistical toolbox and Mapping toolbox. We digitized each water depth of the 1930 and 2002 nautical charts (Figs. 4a and 4b) to evaluate bathymetry changes and shoreline changes of the western Taiwan coast at decadal intervals (Figs. 5b and 5e). We placed the western edge of the subaqueous SWTD at the 40 m or 100 m isobath (red lines in Figs. 5c and 5f) to mark the seaward edge (zero thickness) of the delta bottomset beds (Fig. 2, pink area).

3.2 Sediment volume and paleo-bathymetry evaluation on a millennial timescale

We constructed and analyzed digital elevation models derived from Shuttle Radar Topography Mission (SRTM) data, ^{14}C dates of borehole cores from the delta, and bathymetric and lithologic core data to make determinations of sediment storage in the SWTD. To accurately measure the delta volume in southwestern Taiwan, we made use of data from 80 cores and 112 ^{14}C dates from previous studies (Chen et al., 2010; Lu, 2006) and the Central Geological Survey, Taiwan. The ^{14}C ages were calibrated using CALIB 7.0 and marine reservoir ages from Yoneda and Uno (2007), and the paleotopography as of 2 cal ka BP and 7 cal ka BP was reconstructed. We referred the core descriptions from hydrogeological data bank, MOEA, Taiwan, ROC (http://hydro.moeacgs.gov.tw/index.htm; in Chinese). The present-day bathymetry (Ocean Data Bank, Institute of Oceanography, National Taiwan University) is combined with the SRTM 3 arc-second topographic data (http://www2.jpl.nasa.gov/srtm/) in Fig. 6a.

We used the modern topography generated by SRTM and bathymetric data to identify subaerial and subaqueous delta regions (Fig. 6a). We determined that the area of the whole delta (Figs. 6b and 6c) is 6646 km^2, consisting of a subaerial delta of 4693 km^2 and a subaqueous delta of 1953 km^2. For the convenience of comparisons, the area was set to be the same in every logical perspective, leaving only input parameters variable. The sediment thickness was defined as zero along the western boundary of the study area, and the area higher than 100 m on the eastern boundary of area was considered as the point of zero thickness for the delta topset beds (Figs. 6b and 6c).

To assess the sediment storage in the SWTD, the volumes of the subaerial and subaqueous deltas were calculated from 7 cal ka BP to the present by using MATLAB. Volumes were converted to masses by using a dry bulk density of 1.6 g/cm^3 based on in situ measurements (Liu et al., 2008). We used sediment discharge data for the eight rivers feeding the SWTD in calculations of the deltaic volume since 7 cal ka BP. Parameters such as gradient and length of the eight rivers were obtained mainly from the Water Resources Agency of Taiwan (Table 1). The 2-ka and 7-ka shorelines were determined as the 0 m level of the paleo-topography considering Holocene changes in sea level. We neglected the effects of sediment compaction and tectonic uplift or subsidence. Finally, we evaluated the volumes of delta sediment at millennial intervals over the last 7 cal ka and at decadal intervals since 1930.

4. Results

4.1 Morphological and shoreline changes on a decadal timescale

Our evaluation showed that between 1930 and 2002, the shoreline migrated landward and removed about 132.33 km^2 of the subaerial SWTD at an average rate of 1.83 km^2 per year (Fig. 4c). The shift in the low-tide lines shows a clear southward shift of the Waisandin Sandbar (Fig. 4c). The shoreline did not change much near Kaohsiung. Other historical maps also document a retreating shoreline over the past three decades (Hsu et al., 2007; http://gissrv4.sinica.edu.tw/gis/twhgis_zh_TW.aspx#).

The Taiwan Strait and South China Sea shelf off the SWTD are relatively narrow (Fig. 2), so for calculation purposes we held the area of the subaqueous delta region constant at 1953.30 km^2 and used the water depths in the nautical charts to estimate the rate and magnitude of the sediment-volume changes in the subaqueous SWTD for the 1930–2002 and 2002–2010 intervals. Between 1930 and 2002, the average annual sediment-volume loss was 8.07 ± 0.43 km^3 (Fig. 5c), corresponding to a deepening rate of 5.74 ± 0.30 cm/y. Between 2002 and 2010, the annual sediment-volume loss was 2.99 ± 0.21 km^3 (Fig. 5f) and the deepening rate was 15.30 ± 1.08 cm/y. The results of inconsistent deepening rates and sediment-volume loss rate indicate deepening bathymetry in response to a dominantly erosional environment during the last seven decades.

4.2 Shoreline changes and sediment trapping on a millennial timescale

The sediment storage within deltaic deposits since 2 cal ka BP amounted to 60.14 ± 7.40 km^3 or an average sediment thickness of about 8.2 m (Fig. 6b). Storage since 7 cal ka BP was 201.72 ± 13.90 km^3 for an average thickness of about 28.2 m (Fig. 6c). The depocenter was at the mouth of the Tsengwen River at both during 0–2 cal ka BP and 0–7 cal ka BP (Figs. 6b and 6c), where sediment deposition reached a maximum of ~75.1 m since 7 cal ka BP (calculated from core TN-TN, Table 2). Several small depocenters with sediment fill more than 50 m thick are distributed along the coast south of the Tsengwen River. The second largest depocenter is at the mouth of the Choshui River, where a maximum of ~52.9 m of sediment has accumulated since 7 cal ka BP (calculated from core CH-HA, Table 2). However, since 2 cal ka BP this depocenter has been less localized, displaying an elongated distribution along the coast (Fig. 6b).

Based on our evaluations of sediment thickness for the last 2 and 7 cal ka (Figs. 6b and 6c), we reconstructed the paleo-topography as of these dates (Figs. 6e and 6f). The shoreline at 7 cal ka BP closely follows the modern boundary of the western foothills, indicating that the area of the delta plain was limited by the basement geology and topography (Fig. 6f). At 2 cal ka BP, the delta plain expanded westward to the area of the paleo-Choshui river, and the shoreline was about 20 km east of its modern location (Fig. 6e). The area between the modern and 2-ka shorelines is about 1972 km^2, and the area between the 2-ka and 7-ka shorelines is about 1728 km^2 (Fig. 6d). These results show that from 7 to 2 cal ka BP, the SWTD expanded seaward and westward and the shoreline shifted about 20 km seaward. Since 2 cal ka BP, this westward progradation has rapidly increased while the delta has continuously expanded.

Estimated sediment volumes of the subaerial and subaqueous parts of the SWTD are listed in Table 3 at 1-ka intervals for the last 7 cal ka. These are calculated on the basis of the present sea level, because sea level has been approximately stable over that time. A total of 201.72 ± 13.90 km^3 of sediment has been trapped in the SWTD over the last 7 cal ka, indicating accumulation rates of 28.82 ± 1.90 Mm^3/y and 46.11 ± 3.30 Mt/y. Millennial volume changes were slightly higher during 6–7 cal ka BP and 0–2 cal ka BP and slightly lower during 2–5 cal ka BP. The subaerial delta was 20.7–26.4% of the total volume, proportions that were relatively large during 6–7 cal ka BP and 0–1 cal ka BP. The subaqueous delta constituted 73.6–79.3% of the total volume, and the proportion was relatively small during 2–4 cal ka BP. The increasing volume below sea level for the last 5 cal ka, particularly for the last 2 cal ka BP, may imply an increase in sediment supply and discharge, resulting in rapid shoreline migration seaward.

5. Discussion

5.1. Morphological and shoreline changes

Our results clearly document coastal regression due to delta progradation along the western coast of Taiwan for the last 7 ka (Fig. 6). They are concordant with the distribution of prehistoric sites and shell mounds in the Tainan area that contain various proportions of marine and estuarine mollusks (Chang, 1970). Different patterns of sediment accumulation are apparent to the north and south of ca. 23.5°N. In the northern segment, simple delta progradation results in a westward increase in sediment thickness toward the present shoreline, corresponding to the delta front of the Choshui and Peikang rivers. In the southern segment, patches of very thick sediment are found in depocenters along the delta front. Active subsidence and uplift have been well documented in the southern segment, particularly between Tainan and Kaohsiung (Chen and Liu, 2000; Fruneau et al., 2001; Lu, 2006). The Holocene marine and fluvial sediments of the Tainan Tableland, with elevations of 20–30 m, have been uplifted at about 5–7 mm/y during the Holocene (Chen and Liu, 2000). The presence near the tableland of middle Holocene eolian dune sediment 20–25 m below sea level is evidence of subsidence at similar rates (Lu, 2006).

Historical records show that a barrier and lagoon system existed along the coastline near Tainan in the 17th century, referred to by Chang (2000) as the Taijiang Inner Sea. The Tsengwen River emptied into the lagoons of this system. Active subsidence and effective sediment trapping by similar barrier and lagoon systems may account for the thick succession associated with a depocenter at the mouth of the Tsengwen River.

Modern observations show that the shoreline is undergoing minor retreat (Chen and Rau, 1998). The Tsengwen River delta front displays erosional features (Hong et al., 2004). The shoreline retreat of the past three decades is strongly affected by human influences, such as the building of various impoundments in the hills and the construction of artificial sea walls and fish ponds in the coastal zone (Lin, 1996; Hsu et al., 2007). In particular, the southwestward migration and reduction in size of the Waisandin Sandbar are consequences of coastal reclamation projects (Kung et al., 1994; Chen and Rau, 1998). Our analysis also documents this degradation of the shoreline, contrasting an average shoreline migration of about 2 m/y seaward since 7 cal ka with an average migration of 2 m/y landward during the past 70 years.

In our analysis, the sediment volume below sea level decreased from 2–1 cal ka to 1–0 cal ka. In our interpretation, the warm current on the eastern side of Taiwan Strait has affected delta-front sedimentation and dispersed mud to the north (Fig. 7). Our results also show that sediment deposition in recent decades is mainly in the northeastern part of Taiwan Strait (Fig. 5c). The retreating modern shoreline implies that sediment will continue to be dispersed from the SWTD to the north.

5.2. Sediment accumulation in SMR deltas and past sediment discharge

Our analysis indicates that the SWTD has trapped an average of ~46.11 Mt/y of sediment during the last 7 ka, of which 6.58 Mt/y is above sea level and 22.24 Mt/y below sea level (Table 3). These values include bedload materials. In large rivers, bedload is estimated to be ~10% of total sediment load (Milliman and Meade, 1983). However, the proportion of bedload is much greater in SMRs as a result of their steeper gradients and coarser materials, because SMRs are located near the mountainous source regions (Orton and Reading, 1993). The abundance of sand-size and coarser grains in core logs (e.g., Fig. 3) supports this idea.

Kao et al. (2008) estimated that sediment accumulation from the delta front to Taiwan Strait is currently 18 Mt/y (of which 12 ± 10 Mt/y is sand and 6 ± 5 Mt/y is mud) for a set of major Taiwanese rivers that included six "northwestern rivers" (Tanshui, Touchien, Houlung, Taan, Tachia and Wu rivers) and two "middle western rivers" (Choshui and Tsengwen). Our estimated sediment accumulation is ~35.6 Mt/y below sea level in the Choshui, Tsengwen, Yenshui and Erhjen rivers combined. As the "middle western rivers" account for roughly two-thirds of the sediment discharge in the SWTD, we estimate sediment trapping for the middle western rivers to be ~24 Mt/y. This value contains bedload materials and does not include mud deposition in the northern Taiwan Strait. Our estimate is greater than that of Kao et al. (2008). We ascribe the difference to the decrease in bedload transport and sediment trapping in reservoirs for the present data, resulting in the current erosional environment on the delta front and shoreline retreat.

Kao et al. (2008) also show that sand from rivers is trapped in Taiwan Strait, but mud accumulation is far smaller than the mud supply of 42 ± 11 Mt/y, indicating that ~85% of the fluvial mud from the SMRs left the Taiwan Strait and was transported further offshore where it is a significant contributor to sedimentation in the East China Sea. Besides, the sediments in the Taiwan Strait are intensely influenced by mixing process based on the radionuclides profiles (Huh and Su, 1999; Su and Huh, 2002). The modern transportation and deposition of sediments in the Taiwan Strait still need to be clarified.

Hsu et al. (2014) made similar estimates of offshore sediment transport for the Tsengwen and Erhjen rivers and found that 22% of the fluvial sediment supply (30 Mt/y, Tsengwen; 25 Mt/y, Erhjen) has accumulated in the delta front to shelf areas (12.1 Mt/y). Because the delta front of the Tsengwen River is currently erosional (Hong et al., 2004), the sediment must be mainly deposited on the shelf.

Sediment trapping of western Taiwanese rivers from the delta front to the prodelta has been estimated as ~100% for sand and ~15% for mud, and sand has occupied 30% of total sediment input for the last 50 years (Kao et al., 2008). If these proportions are applicable to the last 7 ka, the amount of mud dispersal to the offshore is estimated to be ~36 Mt/y from the "middle western rivers". It will be sure that significant amount of muddy sediment has been transported northward to the East China Sea.

We cannot evaluate the sediment dispersal on a millennial time scale for the Tsengwen and Erhjen rivers; however, if the sediment is partitioned equally within deltas and beyond deltas, and if historical sediment discharges are typical of the Holocene, then offshore sediment dispersal from the Tsengwen and Erhjen rivers would be ~12 Mt/y and delta trapping would also be ~12 Mt/y. Given our limited knowledge of past sediment discharge and dispersal for Taiwanese rivers, further study is needed for a wide region including the East China Sea and South China Sea.

5.3. Sediment trapping and dispersal of SMR deltas in southwest Taiwan

The river-mouth systems of SMRs vary in different settings. In compressional plate settings, rivers commonly feed offshore canyon/gully systems cutting directly across a narrow shelf. The Kaoping River of Taiwan is a good example, in which 50% of fluvial sediments are deposited within 120 km of the river mouth (up to ~2000 m depth beyond the shelf edge), and the rest is dispersed farther away (Kao et al., 2006). Flood-driven hyperpycnal flows or turbidity currents are frequent, and most riverine sediment is transported directly to a deep-sea basin (Liu et al., 2016). Similarly, ~90% of the sediment from the Sepik River of New Guinea and the Kurobe River of central Japan is transported by an offshore canyon (Walsh and Nittrouer, 2003) and gullies (Saito, 2011), respectively. Although the Tsengwen and Erhjen rivers in our study area formed a Holocene delta, at present ~80% of the fluvial sediment discharge is transported beyond the shelf edge (Hsu et al., 2014). After the SWTD was filled up and bypassed, the delta has shifted to a destruction phase (Hong et al., 2004). The shelf is also narrow off these rivers, measuring <30 km from the shore to the shelf edge or the Penghu Channel.

The SWTD lies on a relatively wide shelf, but the Taiwan Warm Current (TwWC) flows near shore. In the eastern Taiwan Strait, sediment trapping between the delta front and prodelta during the last 50 years has captured almost all of the sand and ~15% the mud from the SWTD (Kao et al., 2008). Most of the mud instead is transported by the TwWC to the East China Sea or beyond. Rivers on the west side of the Taiwan orogen are in a foreland basin or back-arc basin setting. Many other SMR deltas in Southeast Asia occupy these geological settings, for instance north of Java (Rimbaman, 1992; Wolanski and Spagnol, 2000). Well-developed river-dominated deltas trap sediment effectively. Relatively stable island margins also have well-developed delta systems in Southeast Asia, such as the Mahakam and Rajang deltas in Borneo (Staub and Esterle, 1993; Staub et al., 2000; Storms et al., 2005). The Fly, Kikori and Purari rivers entering the Gulf of Papua southeast of New Guinea form deltas and clinoforms; there, most of the sediment discharged by the rivers is trapped in the delta to shelf areas and <5% is transported off the continental shelf (Walsh and Nittrouer, 2003; Walsh et al., 2004).

Tectonic subsidence in southwestern Taiwan accounts for the rapid accumulation of deltaic sediment deposits (Chen and Liu, 2000; Fruneau et al., 2001). More than 70 m has accumulated during the last 7 cal ka, for an average rate of ~10.73 m/ka. Compared to other deltas in foreland or back-arc basin settings, the trapping efficiency of the SWTD is relatively low due to the influence of the TwWC and steep river gradients, but rapid subsidence provides substantial accommodation space within a limited area. The thickness of the deltaic sediments of southwestern Taiwan may indicate high preservation potential since 7 cal ka BP.

5.4. Sediment supply to East China Sea and establishment of modern ocean circulation

As shown by Kao et al. (2008), ~36 Mt/y of muddy sediment delivered by major rivers of western Taiwan for the last 50 years is missing. Mud accumulation on the middle to outer shelf of the ECS is rare (Huh and Su, 1999; Su and Huh, 2002), where active and moribund sand ridges are widely developed at present (Liu et al., 2007b; Wu et al., 2016). Tidal and monsoon-induced currents, reported by in-situ measurement (e.g., Hoshika et al., 2003; Liu et al., 2007b), prevent the accumulation of fine particles on the middle to outer shelf of the ECS, resulting in sediment bypassing on the shelf. Provenance studies of sediment in the Okinawa Trough based on clay mineralogy and geochemical analyses have shown that significant quantities of riverine sediment from northern and eastern Taiwan are transported by the Kuroshio to the middle Okinawa Trough (Dou et al., 2010a, 2010b, 2012; Wang et al., 2015) and by the Tsushima Warm Current (TsWC) to the northern Okinawa Trough (Xu et al., 2012b, 2012c, 2014). However, these studies have presented little basic information on the character of Taiwanese rivers. A basic dataset of Taiwanese rivers (Li et al., 2012a, 2013) has been used to show the similarity between sediments of the western or southwestern Taiwanese rivers and the middle Okinawa Trough (Li et al., 2013) and southern Okinawa Trough (Dou et al., 2016). Figure 8 presents the dates of this abrupt shift at core locations around the East China Sea. The provenance of sediment in cores from the Okinawa Trough and the Japan Sea shifted abruptly to its modern character at 7.1–7.3 cal ka BP. Similarly, an abrupt change in accumulation rates has been reported in the southern and northern Okinawa Trough (Jian et al., 2000). On the other hand, it occurred later (6.0–6.5 cal ka BP) in the Yellow Sea and East China Sea continental shelf. This shift is considered to represent the establishment of the modern ocean current system in the Yellow Sea and East China Sea continental shelf.

The TsWC is a branch of the Kuroshio (Nitani, 1972; Ichikawa and Beardsley, 2002). It is hard to explain the abrupt shift in sediment provenance and accumulation rates under a scenario in which the Kuroshio alone transports sediment from the western Taiwanese rivers. Current monitoring data and simulations show that the TsWC can be linked with the TwWC regularly in summer and episodically in winter (Beardsley et al., 1985; Fang et al., 1991; Ichikawa and Beardsley, 2002; Zhu et al., 2004; Isobe, 2008; Zheng, 2009; Park et al., 2013). The Kuroshio and TwWC are the two dominant sources of water flowing through the Tsushima Strait into the Japan Sea, the TwWC being dominant in summer (66% of the total volume) and the Kuroshio in winter (83%) (Cho et al., 2009).

As the TwWC flows north through the Taiwan Strait into the East China Sea, the bathymetry of the Taiwan Strait is a key factor influencing the birth of the TwWC. The south entrance of the Taiwan Strait is a wide, shallow shoal with water depths of ~10–20 m named the Taiwan Shoal or Taiwan Bank. During the early Holocene lowstand of sea level at –50 m, the Taiwan Strait was restricted to a narrow, sinuous channel only ~20–30 km wide between the South China Sea and East China Sea. The TwWC arose after the rise of sea level and submergence of the Taiwan Shoal to appropriate depths.

Early Holocene sea-level rise took place in three stages: a gradual rise during 13.0–9.0 cal ka BP (Bard et al., 2010; Tjallingii et al., 2014), a rapid rise from 9.0 to 8.2 (or 8.0) cal ka BP (Hori and Saito, 2007; Tamura et al., 2009; Bird et al., 2010; Hijma and Cohen, 2010; Wang et al., 2013; Tjallingii et al., 2014), and a slow rise from 8.0 to 6.5 cal ka BP (Yu et al., 2007; Cronin et al., 2007; Tamura et al., 2009; Hijma and Cohen, 2010; Bird et al., 2010; Li et al., 2012b; Tjallingii et al., 2014). The third stage ended with the final phase of North America deglaciation (Carlson et al., 2007; Lambeck et al., 2014) and is documented by evidence from several regions: ~4 m rise during 7.5–6.5 cal ka BP in Singapore (Bird et al., 2010), ~4.5 m rise at ~7.6 cal ka BP in the Baltic Sea (Yu et al., 2007), ~6 m rise during 8.2–7.6 cal ka BP in Chesapeake Bay (Cronin et al., 2007), ~5 m rise during 8.0–7.1 cal ka BP in the Mekong delta (Tamura et al., 2009; Li et al., 2012b), and a 3.6 m rise during 8.0–7.6 cal ka BP in Kolleru Lake, India (Nageswara Rao et al., submitted). In the Taiwan Strait, sea level reached its present level at 7.0 cal ka BP (Chen and Liu, 1996).

We correlate the abrupt provenance shift in Okinawa Trough sediment with the birth of the TwWC following the early Holocene sea-level rise, after which the TwWC began to deliver sediment derived from western Taiwanese rivers to the East China Sea. The synchronous change of sedimentation along the Okinawa Trough to the Japan Sea is explained by the linkage between the TwWC and TsWC, as is the strengthening of the TsWC. In the other idea on indirect relationship between the TwWC and TsWC, the TwWC flows northward towards the Yangtze River mouth, and the TsWC is only a branch of the Kuroshio (Ichikawa and Beardsley, 2002). In this case, it is hard to explain sediment source and dispersal in the middle to northern Okinawa Trough, and synchronization of the abrupt change at 7.3 cal ka BP.

The abrupt shift in sediment provenance in the Yellow Sea and East China Sea continental shelf occurred slightly later at 6.5–6.0 cal ka BP. The Yellow Sea Warm Current (YSWC), an episodic event forced by northerly winter monsoon winds (Isobe, 2008), can be linked to the strength of the winter monsoon or the direction of northerly winds after the middle Holocene warm period. However, the East Asian Winter Monsoon had a weakening trend from the early to late Holocene with its most significant transition at ~6.2 cal ka BP, in phase with a weakening trend of the East Asian Summer Monsoon (Jia et al., 2015). Thus the rise of the YSWC may instead reflect the changing balance between the winter and summer monsoons, or the stabilization of a further sea-level rise after the birth of the TwWC. The establishment of the modern ocean current system in the Yellow Sea remains a topic in need of explanation.

6. Conclusion

This study showed that the SMRs of western Taiwan have provided a large sediment supply to the coast and also built the thick deltaic deposits of the SWTD in the coastal plain. We used historical charts, bathymetric data, SRTM observations and ^{14}C dates to evaluate the sediment volume in this area on millennial and decadal scales. We calculate that 201.72 ± 13.90 km^3 of stored sediment has accumulated within the SWTD since ~7 cal ka BP. Sediment trapping amounts to an average of 46.11 ± 3.30 Mt/y since ~7 cal ka BP, of which approximately 20–25% has been trapped above sea level. Whereas the paleo-shoreline has steadily prograded on a millennial scale since 7 cal ka BP, the modern shoreline has been eroding landward by about 2 m/y in the last seven decades. Nautical charts document minor reduction in the volume of the offshore delta along with a deepening rate of about 10 cm/y, consistent with an erosional environment during the last seven decades. We ascribe this shoreline retreat to delta destruction in response to human activities. Today a significant portion of the sediment historically supplied by western Taiwanese rivers has been cut off. This sediment was formerly transported northward into the East China Sea after the abrupt birth of the TwWC, which arose after a rapid sea-level rise in the early to middle Holocene. Abrupt changes of sediment provenance in the Okinawa Trough at ~7.3 cal ka BP are explained by the birth of the TwWC, its close link with the TsWC, and its interaction with the Kuroshio.

Acknowledgements

We are grateful to C.A. Huh for constructive comments on sedimentation in the Taiwan Strait. We thank the anonymous reviewer for the helpful comments to improve this paper. This work was financially supported by the National Science Council Overseas Project (NSC-103-2917-I-564-013), Taiwan, and by the JSPS G-8 project (DELTAs). We thank the Central Geological Survey, Taiwan, for providing the ^{14}C data.

References

Bard, E., Hamelin, B., Delanghe-Sabatier, D., 2010. Deglacial Meltwater Pulse 1B and Younger Dryas Sea Levels Revisited with Boreholes at Tahiti. Science 327, 1235–1237.

Beardsley, R.C., Limeburner, R., Yu, H., Cannon, G.A., 1985. Discharge of the Changjiang (Yangtze River) into the East China Sea. Continental Shelf Research 4, 57–76.

Bianchi, T.S., Allison, M.A., 2009. Large-river delta-front estuaries as natural "recorders" of global environmental change. Proceedings of the National Academy of Sciences 106, 8085–8092.

Bird, M.I., Austin, W.E.N., Wurster, C.M., Fifield, L.K., Mojtahid, M., Sargeant, C., 2010. Punctuated eustatic sea-level rise in the early mid-Holocene. Geology 38, 803–806.

Bowin, C., Lu, R.S., Lee, C.S., Schouten, H., 1978. Plate convergence and accretion in Taiwan-Luzon region. American Association of Petroleum Geologists Bulletin, 62, 1645–1672.

Carlson, A.E., Clark, P.U., Raibeck, G.M., Brook, E.J., 2007. Rapid Holocene deglaciation of the Labrador Sector of the Laurentide Ice Sheet. Journal of Climate 20, 5126–5133.

Chang, J.C., 2000. Geomorphological Change on the Tsengwen Coastal Plain in Southwestern Taiwan. In: Slaymaker, O. (Ed.) Geomorphology, human activity and global environmental change. Wiley & Sons, Ltd., pp. 235–247.

Chang, K.C., 1970. Prehistoric Archaeology of Taiwan. Asian Perspectives 13, 59–77.

Chen, H.W., Lee, T.Y., Wu, L.C., 2010. High-resolution sequence stratigraphic analysis of Late Quaternary deposits of the Changhua Coastal Plain in the frontal arc-continent collision belt of Central Taiwan. Journal of Asian Earth Sciences 39, 192–213.

Chen, L.C., Rau, J.Y., 1998. Detection of shoreline changes for tideland areas using multi-temporal satellite images. International Journal of Remote Sensing 19, 3383–3397.

Chen, W.F., Liu, T.K., 2003. Dissolved oxygen and nitrate of groundwater in Choshui Fan-Delta, western Taiwan. Environmental Geology 44, 731–737.

Chen, Y.G., Liu, T.K., 1996. Sea level changes in the last several thousand years, Penghu Islands, Taiwan Strait. Quaternary Research 45, 254–262.

Chen, Y.G., Liu, T.K., 2000. Holocene uplift and subsidence along an active tectonic margin southwestern Taiwan. Quaternary Science Reviews 19, 923–930.

Chern, C.S., Wang, J., 2000. Some aspects of the flow-topography interactions in the Taiwan Strait. Terrestrial Atmospheric and Oceanic Sciences 11, 861–878.

Cho, Y.K., Seo, G.H., Choi, B.J., Kim, S., Kim, Y.G., Youn, Y.H., Dever, E.P., 2009. Connectivity among straits of the northwest Pacific marginal seas. Journal of Geophysical Research 114, C06018.

Cronin, T.M., Vogt, P.R., Willard, D.A., Thunell, R., Halka, J., Berke, M., Pohlman, J., 2007. Rapid sea level rise and ice sheet response to 8,200-year climate event. Geophysical Research Letters 34, L20603.

Dadson, S.J., Hovius, N., Chen, H., Dade, W.B., Hsieh, M.L., Willett, S.D., Hu, J.C., Horng, M.J., Chen, M.C., Stark, C.P., Lague, D., Lin, J.C., 2003. Links between erosion, runoff variability and seismicity in the Taiwan orogeny. Nature 426, 648–651.

Dadson, S.J., Jovius, N., Chen, H., Dade, W.B., Lin, J.C., Hsu, M.L., Lin, C.W., Horng, M.J., Chen, T.C., Milliman, J., Stark, C.P., 2004. Earthquake-triggered increase in sediment delivery from an active mountain belt. Geology 32, 733–736.

Dalrymple, R.W., Baker, E.K., Harris, P.T., Hughes, M.G., 2003. Sedimentology and stratigraphy of a tide-dominated, foreland-basin delta (Fly river, Papua New Guinea). In: Sidi, F.H., Nummendal, D., Imbert, P., Darman, H., Posamentier, H.W. (Eds.), Tropical Deltas of Southeast Asia—Sedimentology, Stratigraphy, and Petroleum Geology, SEPM Special Publication 76, 147–173.

Dou, Y.G., Yang, S.Y., Liu, Z.X., Clift, P.D., Shi, X.F., Yu, H., Berne, S., 2010a. Clay mineral evolution in the middle Okinawa Trough since 28 ka: implications for sediment provenance and paleoenvironmental change. Palaeogeography Palaeoclimatology Palaeoecology 288, 108–117.

Dou, Y.G., Yang, S.Y., Liu, Z.X., Clift, P.D., Shi, X.F., Yu, H., Berne, S., 2010b. Provenance discrimination of siliciclastic sediments in the middle Okinawa Trough since 30 ka: constraints from rare earth element compositions. Marine Geology 275, 212–220.

Dou, Y.G., Yang, S.Y., Liu, Z.X., Shi, X.F., Li, J., Yu, Hua, Berne, S., 2012. Sr–Nd isotopic constraints on terrigenous sediment provenances and Kuroshio Current variability in the Okinawa Trough during the late Quaternary. Palaeogeography Palaeoclimatology Palaeoecology 356–366, 38–47.

Dou, Y., Yang, S., Shi, X., Clift, P.D., Liu, S., Liu, J., Li, C., Bi, L., Zhao, Y., 2016. Provenance weathering and erosion records in southern Okinawa Trough sediments since 28ka: Geochemical and Sr–Nd–Pb isotopic evidences. Chemical Geology 425, 93–109.

Elliott, T., 1978. Deltas. In: Reading, H.G. (Ed.) Sedimentary Environments and Facies. Blackwell Scientific Publication, pp. 97–142.

Fang, G., Zhao, B., Zhu, Y., 1991. Water volume transport through the Taiwan Strait and the continental shelf of the East China Sea measured with current meters. In: Takano, K. (Ed.) Oceanography of Asian Marginal Seas. Elsevier, New York. p. 345–348.

Fang, L., Xiang, R., Zhao, M., Zhou, L., Liu, J., Zhang, L., 2013. Phase evolution of Holocene paleoenvironmental changes in the southern Yellow Sea: Benthic foraminiferal evidence from core C02. Journal of Ocean University of China 12, 629–638.

Fruneau, B., Pathier, E., Raymond, D., Deffontaines, B., Lee, C.T., Wang, H.T., Angelier, J., Rudant, J.R., Chang, C.R., 2001. Uplift of Tainan Table land (SW Taiwan) revealed by SAR interferometry. Geophysical Research Letters 16, 3071–3074.

Galloway, W.E., 1975. Process framework for describing the morphologic and stratigraphic evolution of deltaic depositional systems. In: Broussard, M.L. (Ed.), Deltas, Models for Exploration. Houston Geological Society, pp. 87–98.

Hijma, M.P., Cohen, K.M., 2010. Timing and magnitude of the sea-level jump preluding the 8200 yr event. Geology 38, 275–278.

Ho, C.S., 1988. An introduction to the geology of Taiwan: explanatory text of the geologic map of Taiwan (2nd edition). Central Geological Survey, MOEA, Taiwan, ROC. 192 p.

Hong, E., Huang, T.C., Yu, H.S., 2004. Morphology and dynamic sedimentology in front of the retreating Tsengwen Delta, Southwestern Taiwan. Terrestrial Atmospheric and Oceanic Sciences 15, 565–587.

Hong, H.S., Chai, F., Zhang, C., Huang, B., Jiang, Y., Hu, J., 2011. An overview of physical and biogeochemical processes and ecosystem dynamics in the Taiwan Strait. Continental Shelf Research 31, S3–S12.

Hoshika, A., Tanimoto, T., Mishima, Y., Iseki, K., Okamura, K., 2003. Variation of turbidity and particle transport in the bottom layer of the East China Sea. Deep-Sea Research II 50, 443–455.

Hori, K., Saito, Y., 2007. An early Holocene sea-level jump and delta initiation. Geophysical Research Letters 34, L18401.

Hovius, N., Stark, C.P., Chu, H.T., Lin J.C., 2000. Supply and Removal of Sediment in a Landslide: Dominated Mountain Belt: Central Range, Taiwan. The Journal of Geology 108, 73–89.

Hsu, F.H., Su, C.C., Wang C.H., Lin, S., Liu, J., Huh, C.A., 2014. Accumulation of terrestrial organic carbon on an active continental margin offshore southwestern Taiwan: Source-to-sink pathways of river-borne organic particles. Journal of Asian Earth Sciences 91, 163–173.

Hsu, T.W., Lin, T.Y., Tseng, I.F., 2007. Human impact on coastal erosion in Taiwan. Journal of Coastal Research 23, 961–973.

Hu, B.Q., Yang, Z., Qiao, S., Zhao, M., Fan, D., Wang, H., Bi, N., Li, J., 2014. Holocene shifts in riverine fine-grained sediment supply to the East China Sea Distal Mud in response to climate change. The Holocene 24, 1253–1268.

Huh, C.A., Su, C.C., 1999. Sedimentation dynamics in the East China Sea elucidated from ^{210}Pb, ^{137}Cs and ^{239,240}Pu. Marine Geology 160, 183–196.

Huh, C.A., Su, C.C., Wang, C.H., Lee, S.Y., Lin, I.T., 2006. Sedimentation in the Southern Okinawa Trough—Rates, turbidites and a sediment budget. Marine Geology 231, 129–139.

Huh, C.A., Chen, W., Hsu, F.H., Su, C.C., Chiu, J.K., Lin, S., Liu, C.S, Huang, B.J., 2011. Modern (<100 years) sedimentation in the Taiwan Strait: Rates and source-to-sink pathways elucidated from radionuclides and particle size distribution. Continental Shelf Research 31, 47–63.

Ichikawa, H., Beardsley, R.C., 2002. The current system in the Yellow and East China Seas. Journal of Oceanography 58, 77–92.

Isobe, A., 2008. Recent advances in ocean-circulation research on the Yellow Sea and East China Sea shelves. Journal of Oceanography 64, 569–584.

Jan, S., Wang, J., Chern, C.S., Chao, S.Y., 2002. Seasonal variation of the circulation in the Taiwan Strait. Journal of Marine Systems 35, 249–268.

Jia, G., Bai, Y., Yang, X., Xie, L., Wei, G., Ouyang, T., Chu, G., Liu, Z., Peng, P., 2015. Biogeochemical evidence of Holocene East Asian summer and winter monsoon variability from a tropical maar lake in southern China. Quaternary Science Reviews 111, 51–61.

Jian, Z., Wang, P., Saito, Y., Wang, J., Pflaumann, U., Oba, T., Cheng, X., 2000. Holocene variability of the Kuroshio current in the Okinawa Trough, northwestern Pacific Ocean. Earth and Planetary Science Letters 184, 305–319.

Kao, S.J., Milliman, J.D., 2008, Water and Sediment Discharge from Small Mountainous Rivers, Taiwan: The Roles of Lithology, Episodic Events, and Human Activities. The Journal of Geology 116, 431–448.

Kao, S.-J., Shiah, F.-K., Wang, C.-H, Liu, K.-K., 2006. Efficient trapping of organic carbon in sediments on the continental margin with high fluvial sediment input off southwestern Taiwan. Continental Shelf Research 26, 2520–2537.

Kao, S.J., Jan, S., Hsu, S.C., Lee, T.Y., Dai, M., 2008. Sediment budget in the Taiwan Strait with high fluvial sediment inputs from mountainous rivers: New observations and synthesis. Terrestrial Atmospheric and Oceanic Sciences 19, 525–546.

Kim, J. M., Kennett, J. P., 1998. Paleoenvironmental changes associated with the Holocene marine transgression, Yellow Sea (Hwanghae). Marine Micropaleontology 34, 71–89.

Kung C.S., Stive, M., Toms, G., 1994. Geomorphological analysis of a beach and sandbar system. Coastal Engineering Proceedings 24, 1837–1848.

Lambeck, K., Rouby, H., Purcell, A., Sun, Y.Y., Sambridge, M., 2014. Sea level and global ice volumes from the Last Glacial Maximum to the Holocene. Proceedings of the National Academy of Sciences of the United States of America 111, 15296–15303.

Li, C.S., Shi, X.F., Kao, S.-J., Chen, M.-T., Liu, Y.G., Fang, X.S., Lv, H.H., Zou, J.J., Liu, S.F., Qiao, S.Q., 2012a. Clay mineral composition and their sources for the fluvial sediments of Taiwanese rivers. Chinese Science Bulletin 57, 673–681.

Li, C.S., Shi, X.F., Kao, S.J., Liu, Y.G., Lyu, H.H., Zou, J.J., Liu, S.F., Qiao, S.Q., 2013. Rare earth elements in fine-grained sediments of major rivers from the high-standing island of Taiwan. Journal of Asian Earth Sciences 69, 39–47.

Li, J., Hu, B., Wei, H., Zhao, J., Zou, L., Bai, F., Dou, Y., Wang, L., Fang, X., 2014. Provenance variations in the Holocene deposits from the southern Yellow Sea: clay mineralogy evidence. Continental Shelf Research 90, 41–51.

Li, T.G., Li, S.Q., Cang, S.X., et al., 2000. Paleo-hydrological reconstruction of the Southern Yellow Sea inferred from foraminiferal fauna in Core YSDP102. Oceanologia et Limnologia Sinica 31, 588–595.

Li, Y.H., 1976. Denudation of Taiwan Island since the Pliocene Epoch. Geology 4, 105–107.

Li, Z., Saito, Y., Mao, L., Tamura, T., Li, Z., Song, B., Zhang, Y.L., Lu, A.Q., Sieng, S., Li, J., 2012b. Mid-Holocene mangrove succession and its response to sea-level change in the upper Mekong River delta, Cambodia. Quaternary Research 78, 386–399.

Liao, H.R., Yu, H.S., 2005. Morphology, hydrodynamics and sediment characteristics of the Changyun Sand Ridge offshore western Taiwan. Terrestrial Atmospheric and Oceanic Sciences 16, 621–640.

Lin, C.C., 1969. Holocene geology of Taiwan. Acta Geologica Taiwanica, Science Reports of the National Taiwan University 13, 83–126.

Lin, G.W., Chen, H., Chen, Y.H., Horng, M.J., 2008. Influence of typhoons and earthquakes on rainfall-induced landslides and suspended sediments discharge. Engineering Geology 97, 32–41.

Lin, J.C., 1996. Coastal modification due to human influence in couth-western Taiwan. Quaternary Science Reviews 15, 895–900.

Liu, J., Saito, Y., Wang, H., Yang, Z., Nakashima, R., 2007a. Sedimentary evolution of the Holocene subaqueous clinoform off the Shandong Peninsula in the Yellow Sea. Marine Geology 236, 165–187.

Liu, Z., Berne, S., Saito, Y., Yu, H., Trentesaux, A., Uehara, K., Yin, P., Liu, J.P., Li, C., 2007b. Internal architecture and mobility of tidal sand ridges in the East China Sea. Continental Shelf Research 27, 1820–1834.

Liu, J.P., Liu, C.S., Xu, K.H., Milliman, J.D., Chiu, J.K., Kao, S.J., Lin, S.W., 2008. Flux and fate of small mountainous rivers derived sediments into the Taiwan Strait. Marine Geology 256, 65–76.

Liu, J.P., Xue, Z., Ross, K., Wang, H.J., Yang, Z.S., Li, A.C., Gao, S., 2009. Fate of sediments delivered to the sea by Asian large rivers: long-distance transport and formation of remote alongshore clinothems. The Sedimentary Record 7(4), 4–9.

Liu, J.T., Hsu, R.T., Hung, J.J., Chang, Y.P., Wang, Y.H., Rendle-Bühring, R.H., Lee, C.L., Huh, C.A., Yang, R.J., 2016. From the highest to the deepest: The Gaoping River–Gaoping Submarine Canyon dispersal system. Earth-Science Reviews 153, 274–300.

Liu, S.F., Shi, X.F., Fang, X.S., Dou, Y.G., Liu, Y.G., Wang, X.C., 2014. Spatial and temporal distributions of clay minerals in mud deposits on the inner shelf of the East China Sea: Implications for paleoenvironmental changes in the Holocene. Quaternary International 349, 270–279.

Lu, C.C. 2006. Stratigraphy and tectonics of southwestern plain of Taiwan since the Last Glacial Epoch. Master Thesis. Institute Applied Geology, National Central University, Taiwan, ROC. 143pp.

Milliman, J.D., Farnsworth, K.L., 2011. Runoff, erosion and delivery to the coastal ocean. River Discharge to the Coastal Ocean: A global synthesis. Cambridge University Press, 333p.

Milliman, J.D., Meade, R.H., 1983. World-wide delivery of river sediment to the oceans. The Journal of Geology 91, 1–21.

Milliman, J.D., Farnsworth, K.L., Albertin, C.S., 1999. Flux and fate of fluvial sediments leaving large islands in the East Indies. Journal of Sea Research 41, 97–107.

Milliman, J.D., Lin, S.W., Kao, S.J., Liu, J.P., Liu, C.S., Chiu, J.K., Lin, Y.C., 2007. Short-term changes in seafloor character due to flood-derived hyperpycnal discharge: Typhoon Mindulle, Taiwan, July 2004. Geology 35, 779–782.

Nageswara Rao, K., Pandey, S., Kubo, S., Saito, Y., Naga Kumar, K.Ch.V., Demudu, D., Hema Milini, B., Nakashima, R., Sadakata, N., submitted. Holocene sea-level changes and LGM climate along the east coast of India inferred from multi-proxy analysis of core sediments from Kolleru Lake. Journal of Quaternary Science.

Nitani, H., 1972. Beginning of the Kuroshio. In: Stommel, H., Yoshida, K. (Eds.) Kuroshio, its physical aspects. University of Tokyo Press, Tokyo, pp. 353–369.

Olariu, C., 2014. Autogenic process change in modern deltas. In: Martinius, A.W., Ravnås, R., Howell, J.A., Steel, R.J., Wonham, J.P. (Eds.) From Depositional Systems to Sedimentary Successions on the Norwegian Continental Margin. John Wiley & Sons, Ltd., pp. 149–166.

Orton, G.J., Reading, H.G., 1993. Variability of deltaic processes in terms of sediment supply, with particular emphasis on grain size. Sedimentology 40, 475–512.

Park, Y.G., Yeh, S.W., Hwang, J.H., Kim, T., 2013. Origin of the Tsushima Warm Current in a high resolution ocean circulation model. Journal of Coastal Research, SI 65, 2041–2046.

Rimbaman, I., 1992. The role of sea-level changes on the coastal environment of northern West Java (case study of Eretan, Losarang and Indramayu). Journal of Southeast Asian Earth Sciences 7, 71–77.

Saito, Y., 2011. Delta-front morphodynamics of the Kurobe river fan-delta, central Japan. River, Coastal and Estuarine Morphodynamics: RCEM 2011, Tsinghua University Press, pp. 506–501.

Shyu, J. B.H., Sieh, K, Chen, Y.G., Liu, C.S., 2005. The neotectonic architecture of Taiwan and its implications for future large earthquakes. Journal of Geophysical Research 110, B08402.

Smith, D.E., Harrison, S., Jordan, J.T., 2011. The early Holocene sea level rise. Quaternary Science Reviews 30, 1846–1860.

Song, B., Li, Z., Saito, Y., Okuno, J., Lu, A.Q., Hua, D., Li, J., Li, Y.X., Nakashima, R., 2013. Initiation of the Changjiang (Yangtze) delta and its response to the mid-Holocene sea level change. Palaeogeography Palaeoclimatology Palaeoecology 388, 81–97,

Stanley, D.J., Warne, A.G., 1994. Worldwide initiation of Holocene marine deltas by deceleration of sea-level rise. Science 265, 228–231.

Staub, J.R., Esterle, J.S., 1993. Provenance and sediment dispersal in the Rajang River delta/coastal plain system, Sarawak, East Malaysia. Sedimentary Geology 85, 191–201.

Staub, J.R., Among, H.L., Gastaldo, R.A., 2000. Seasonal sediment transport and deposition in the Rajang River delta, Sarawak, East Malaysia. Sedimentary Geology 133, 249–264.

Storms, J.E.A., Hoogendoom, R.M., Dam, R.A.C., Hoitink, A.J.F., Kroonenberg, S.B., 2005. Late-Holocene evolution of the Mahakam delta, East Kalimantan, Indonesia. Sedimentary Geology 180, 149–166

Su, C.C., Huh, C.A. 2002. ^{210}Pb, ^{137}Cs and ^{239,240}Pu in East China Sea sediments: sources, pathways and budgets of sediments and radionuclides. Marine Geology, 183, 163–178.

Syvitski, J., 2003. Sediment fluxes and rates of sedimentation. In: Middleton, G. V. (Ed.), Encyclopedia of Sediments and Sedimentary Rocks. Dordrecht: Kluwer Academic Publishers, pp. 600–606.

Taira, K., 1975. Holocene crustal movements in Taiwan as indicated by radiocarbon dating of marine fossils and driftwood. Tectonophysics 28, T1–T5.

Tamura, T., Saito, Y., Sieng, S., Ben, B., Kong, M., Sim, I., Choup, S., Akiba, F., 2009. Initiation of the Mekong River delta at 8 ka: evidence from the sedimentary succession in the Cambodian lowland. Quaternary Science Reviews 28, 327–344.

Teng, L.S., 1990. Geotectonic evolution of late Cenozoic arc-continent collision in Taiwan. Tectonophysics 183, 57–76.

Tjallingii, R., Stattegger, K., Stocchi, P., Saito, Y., Wetzel, A., 2014. Rapid flooding of the southern Vietnam shelf during the early to mid-Holocene. Journal of Quaternary Science 29, 581–588.

Um, I.K., Choi, M.S., Lee, G.S., Chang, T.S., 2015. Origin and depositional environment of fine-grained sediments since the last glacial maximum in the southeastern Yellow Sea: evidence from rare earth elements. Geo-Marine Letters 35, 421–431.

Walsh, J.P., Nittrouer, C.A., 2003. Contrasting styles of off shelf sediment accumulation in New Guinea. Marine Geology 196, 105–125.

Walsh, J.P., Nittrouer, C.A., Palinkas, C.M., Ogston, A.S., Sternberg, R.W., Brunskill, G.J., 2004. Clinoform mechanics in the Gulf of Papua, New Guinea. Continental Shelf Research 24, 2487–2510.

Wang, H., Saito, Y., Zhang, Y., Bi, N., Sun, X., Yang Z., 2011. Recent changes of sediment flux to the western Pacific Ocean from major rivers in East and Southeast Asia. Earth-Science Reviews 108, 80–100.

Wang, J., Li, A.C., Xu, K.H., Zheng, X.F., Huang, J., 2015. Clay mineral and grain size studies of sediment provenances and paleoenvironment evolution in the middle Okinawa Trough since 17 ka. Marine Geology 366, 49–61.

Wang, Y.H., Jan, S., Wang, D.P., 2003. Transports and tidal current estimates in the Taiwan Strait from shipboard ADCP observations (1999–2001). Estuarine, Coastal and Shelf Science 57, 193–199.

Wang, Y.H., Li, G.X., Zhang, W.G., Dong, P., 2014. Sedimentary environment and formation mechanism of the mud deposit in the central South Yellow Sea during the past 40 kyr. Marine Geology 347, 123–135.

Wang, Z.H., Zhan, Q., Long, H.Y., Saito, Y., Gao, X.Q., Wu, X.X., Li, L., Zhao, Y.N., 2013. Early to mid-Holocene rapid sea-level rise and coastal response on the southern Yangtze delta plain, China. Journal of Quaternary Science 28, 659–672.

Wilson, C.A., Goodbred, S.L.Jr., 2015. Construction and maintenance of the Ganges-Brahmaputra-Meghna Delta: Linking process, morphology, and stratigraphy. Annual Review of Marine Science 7, 67–88.

Wolanski, E., Spagnol, S., 2000. Environmental degradation by mud in tropical estuaries. Regional Environmental Chnage 1, 152–162.

Woodroffe, C.D., Saito, Y., 2011. River-dominated coasts. In: Wolanski, E., McLusky, D.S. (Eds.) Treatise of Estuarine and Coastal Science, Volume 3, Chapter 5, Academic Press, pp. 117–135.

Woodroffe, C.D., Nicholls, R.J., Saito, Y., Chen, Z., Goodbred, S.L., 2006. Landscape Variability and the Response of Asian Megadeltas to Environmental Change. In: Harvey, N. (Ed.), Global Change and Integrated Coastal Management, Springer, pp. 277–314.

Wright, L.D., 1977. Sediment transport and deposition at river mouths: A synthesis. Geological Society of America Bulletin 88, 857–868.

Wu, Z., Jin, X., Zhou, J., Zhao, D., Shang, J., Li, Z., Cao, Z., Liang, Y., 2016.

Comparison of buried sand ridges and regressive sand ridges on the outer shelf of the East China Sea. Marine Geophysical Research, DOI 10.1007/s11001-016-9278-z
Xu, K., Milliman, J.D., Li, A., Liu, J.P., Kao, S.J., Wan, S., 2009. Yangtze- and Taiwan-derived sediments on the inner shelf of East China Sea. Continental Shelf Research 29, 2240–2256.
Xu, K., Li, A., Liu, J.P., Milliman J.D., Yang, Z., Liu, C.S., Kao, S.J., Wan, S., Xu, F., 2012a. Provenance, structure, and formation of the mud wedge along inner continental shelf of the East China Sea: A synthesis of the Yangtze dispersal system. Marine Geology 291–294, 176–191.
Xu, Z.K., Li, T.G., Chang, F.Q., Choi, J.Y., Lim, D.I., Xu, F.J., 2012b. Sediment provenance discrimination in northern Okinawa Trough during the last 24 kyr BP and paleoenvironmental implication: rare earth elements evidence. Journal of Rare Earths 30, 1184–1190.
Xu, Z.K., Li, T.G., Nan, Q.Y., Yu, X.K., Li, A.C., Choi, J.Y., 2012c. Paleoenvironmental changes in the northern Okinawa Trough since 25 kyr BP: REE and organic carbon evidence. Journal of Earth Science 23, 297–310.
Xu, Z.K., Lim, D.G., Choi, J.Y., Li, T.G., Wan, S.M., Rho, K.C., 2014. Sediment provenance and paleoenvironmental change in the Ulleung Basin of the East (Japan) Sea during the last 21 kyr. Journal of Asian Earth Sciences 93, 146–157.
Yang, L., Su, J.A., 2001. Modeling Pollution of a Coastal Lagoon in Taiwan. Journal of Coastal Research 34, 388–396.
Yoneda, M., Uno, H., 2007. Radiocarbon marine reservoir ages in the western Pacific estimated by pre-bomb molluscan shells. Nuclear Instruments and Methods in Physics Research B 259, 432–437.
Yu, H.S., Huang, Z.Y., 2003. Morphology and geologic implications of Penghu Channel off southwest Taiwan. Terrestrial Atmospheric and Oceanic Sciences 14, 469–485.
Yu, S.Y., Berglund, B.E., Sandgren, P., 2007. Evidence for a rapid sea-level rise 7600 yr ago. Geology 35, 891–894.
Zheng, P.N., 2009. The relationship between the Taiwan Warm Current and Tsushima Warm Current. Journal of Hydrodynamics 21, 212–218.
Zhu, J., Chen, C., Ding, P., Li, C., Lin, H., 2004. Does the Taiwan warm current exist in winter? Geophysical Research Letters 31, L12302.

Figure and Table captions

Fig. 1. Location map showing topography, bathymetry, and catchments and deltas

(subaerial and subaqueous) in western Taiwan. The inset map shows the regional setting. Eight small mountainous rivers flowing westward across the subaerial delta are numbered as follows: 1, Choshui; 2, Peikang; 3, Potzu; 4, Pachang; 5, Chishui; 6, Tsengwen; 7, Yenshui; 8, Erhjen (see Table 1). Upland catchments are shown for the Choshui and Tsengwen rivers. Major structure lines (brown) are identified as follows: a, Chukou fault; b, Lishan fault; c, Chauzhou fault; d, Laonung fault; e, Chiuchih fault; f, Chelungpu fault; g, Changhua fault; h, Longitudinal Valley suture. The study area is outlined by the box and enlarged in Figs. 4, 5 and 6. Topography in the catchment areas is omitted.

Fig. 2. Map showing regional bathymetry (contour interval 10 m) and main morphological features of Taiwan Strait near western Taiwan. The subaqueous delta is separated into northern (green) and southern parts (pink). The northern subaqueous delta is a narrow belt about 10 km wide on a relatively flat shelf east of the Changyun sand ridges. The southern subaqueous delta extends along a narrow shelf east of the Penghu Channel and has a relatively steep distal slope. Red triangles are borehole core sites on land, the black square is core site TN-SF. The Changyun sand ridges and depocenters (blue) are modified from Liao et al. (2005) and Liu et al. (2008).

Fig. 3. Simplified lithostratigraphic section of core TN-SF (location in Fig. 2) showing facies successions from latest Pleistocene to Holocene and calibrated ^{14}C ages. Interpolated ages of 2 cal ka BP and 7 cal ka BP are placed at 9.62 m and 46.30 m core depth, respectively. The base of an upward-coarsening deltaic succession in the marine facies is identified at 7 cal ka BP (Lu, 2006).

Fig. 4. (a) Nautical chart of the study area circa 1930 compiled from surveys by the Imperial Japanese Navy (charts 088632, 088633, 088640 and 088706). (b) Nautical chart of the study area circa 2002 compiled from Taiwanese surveys (charts 3231 and 2409). (c) Shorelines and low tide lines derived from the 1930 and 2002 charts. Note the changing position of the Waisandin Sandbar (WS).

Fig. 5. (a) Nautical chart of the study area circa 1930 showing the shoreline and low tide line. (b) Regional bathymetry digitized from Fig. 5a. (c) Changes in bathymetry between 1930 and 2002. (d) Nautical chart circa 2002 showing the shoreline and low tide line. (e) Regional bathymetry digitized from Fig. 6a. (f) Changes in bathymetry between 2002 and 2010. The red line in (c) and (f) is the western boundary of the delta, which is the same with Fig. 6.

Fig. 6. Maps showing present and inferred paleo-topography and paleo-bathymetry of the study area. (a) Modern topography (from SRTM data) and bathymetry (from 2010 data). Core sites are marked by red triangles. (b) Isopach map of deltaic

sediment deposited since 2 cal ka BP. (c) Isopach map of deltaic sediment deposited since 7 cal ka BP. Both (b) and (c) are based on 80 core samples with 112 ^{14}C ages. (d) Locations of the modern shoreline (red line) and paleo-shorelines (dotted lines). (e) Reconstructed paleo-topography and paleo-bathymetry at 2 cal ka BP. (f) Reconstructed paleo-topography and paleo-bathymetry at 7 cal ka BP.

Fig. 7. (a) Map showing regional sediment transport, surface currents and the distribution of mud around the Taiwan Strait (modified from Jan et al., 2002; Liu et al., 2008; and Xu et al., 2009). (b) Map showing the distribution of surficial sediment in the eastern Taiwan Strait (modified from Liao et al., 2005; Huh et al., 2011; and K. Xu et al., 2012).

Fig. 8. Regional bathymetric map showing schematic ocean circulation during summer in the Yellow Sea and East China Sea and ages of abrupt changes in sediment sources (cal ka BP and core name). Red arrows depict the directions and magnitudes of currents, including the interaction between the Taiwan Warm Current (TwWC) and the Kuroshio resulting in the formation of the Tsushima Warm Current (TsWC). Currents are modified after Isobe (2008) and Hong et al. (2011). Age data are from Yellow Sea cores NYS-101 and 102 (Liu et al., 2007a, 2009), B-L44 and B-U35 (Li et al., 2012a), HMB-102 and HMB-103 (Um et al., 2015), YSC-1 and YSC-4 (Li et al., 2014), C02 (Fang et al., 2013), CC02 and DH4-1 (Kim and Kennett, 1998), YS01A (Wang et al., 2014), and DSDP102 (Li et al., 2000), Japan Sea core ROV07-2 (Xu et al., 2014), East China Sea shelf cores MZ02 (Liu et al., 2014) and B3 (Hu et al., 2014), and Okinawa Trough cores B-3GC, 255 (Jian et al., 2000), PC-1 (Xu et al., 2012a; Xu et al., 2014), CSH1 (Xu et al., 2012b), OKI04 (Wang et al., 2015), DGKS9604 (Duo et al., 2010b; 2012; Li et al., 2013), and 1202B (Duo et al., 2016). Core 1202B is located in the south flank of the Okinawa Trough, therefore the influence of the TwWC is not clear.

Table 1. Summary of the eight small mountainous rivers in the west and southwest Taiwan.

Table 2 ^{14}C data in the study area in the west and southwest Taiwan. Core descriptions and related information are collected from hydrogeological data bank, MOEA, Taiwan, ROC. http://hydro.moeacgs.gov.tw/index.htm.

Table 3 The total volumes and partial volumes above/below the present sea level of the Southwest Taiwan Delta.

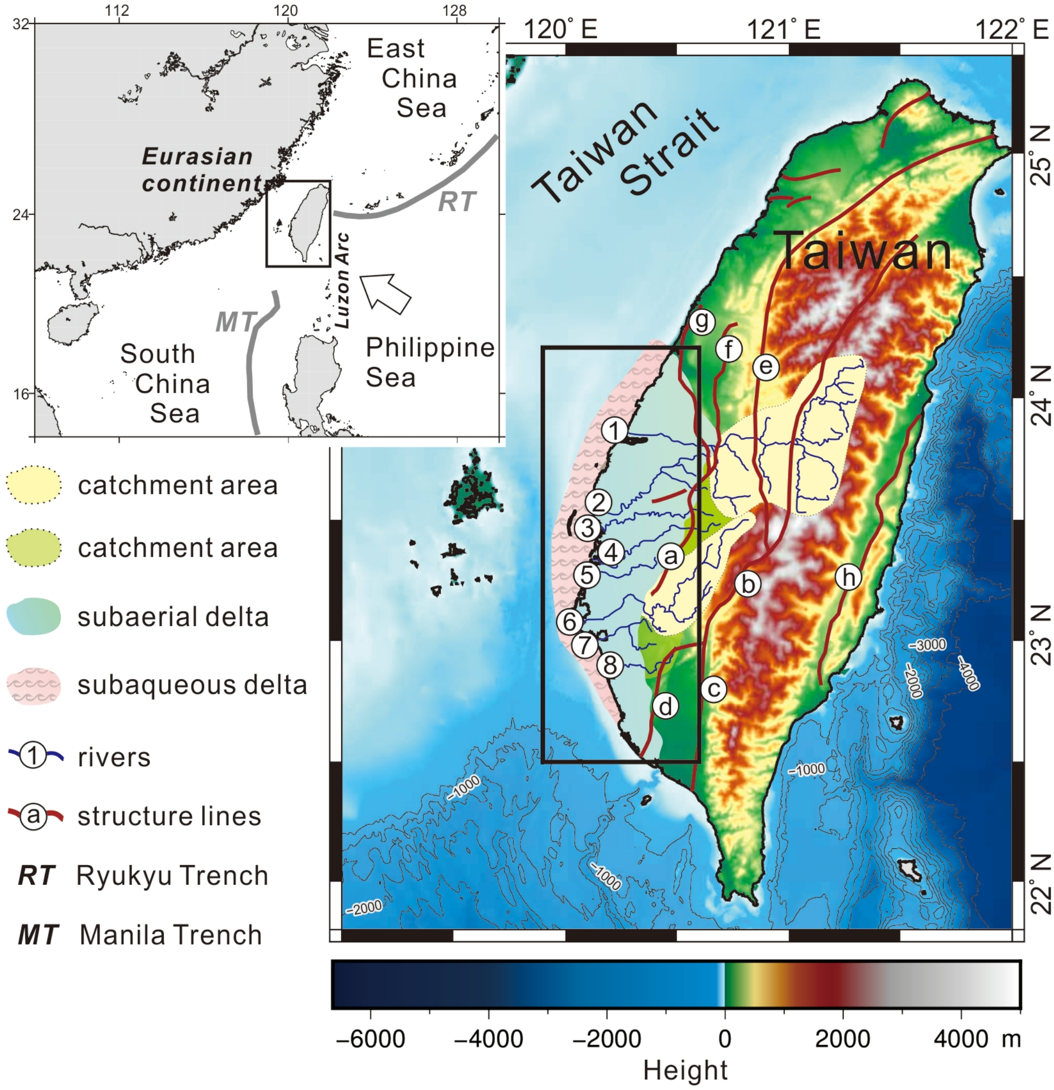

East China Sea
Eurasian continent
RT
MT
Luzon Arc
South China Sea
Philippine Sea
Taiwan Strait
Taiwan
120° E
121° E
122° E
25° N
24° N
23° N
22° N
catchment area
catchment area
subaerial delta
subaqueous delta
rivers
structure lines
RT Ryukyu Trench
MT Manila Trench
−6000
−4000
−2000
0
2000
4000 m
Height

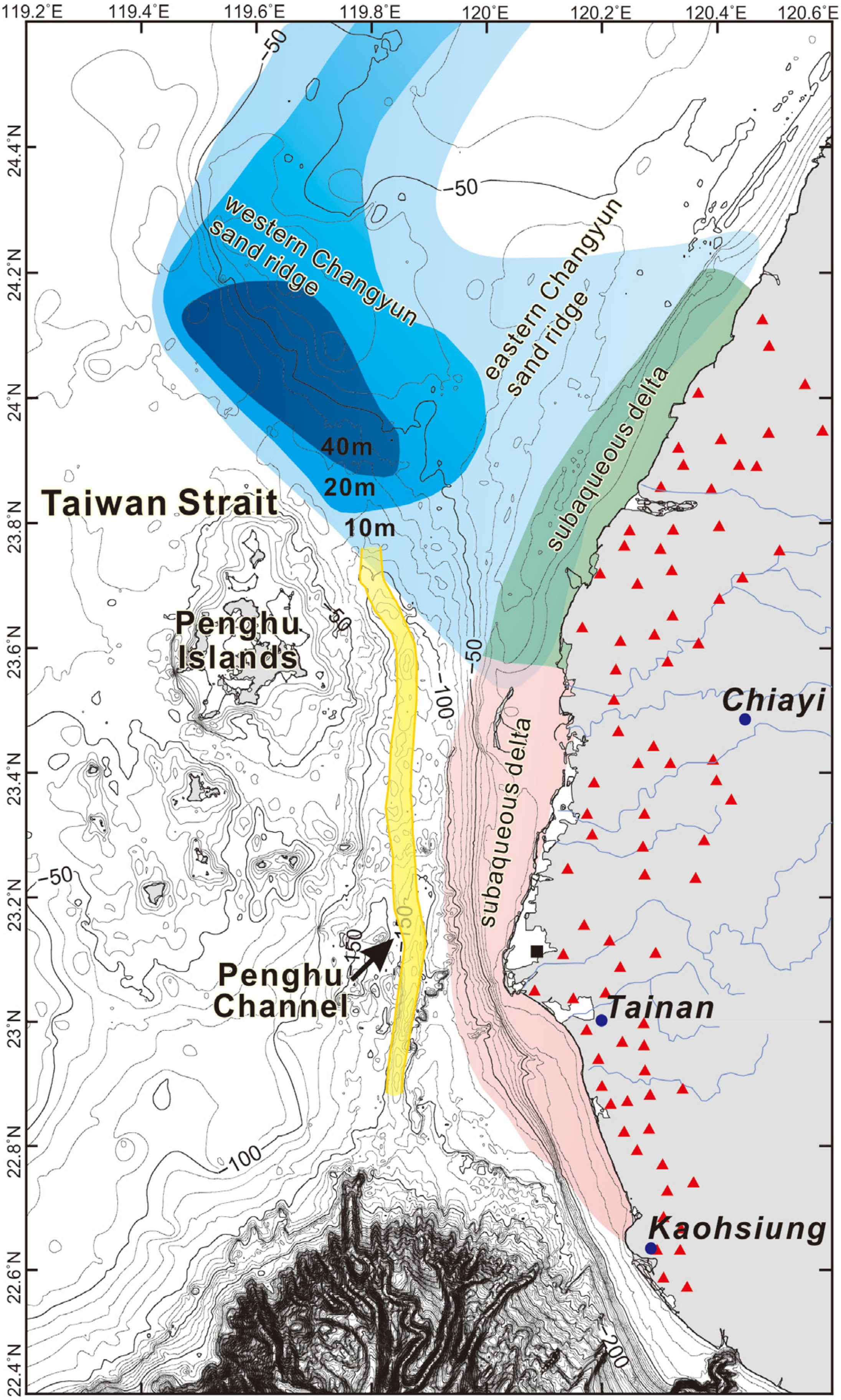

119.2˚E
119.4˚E
119.6˚E
119.8˚E
120˚E
120.2˚E
120.4˚E
120.6˚E
24.4˚N
24.2˚N
24˚N
23.8˚N
23.6˚N
23.4˚N
23.2˚N
23˚N
22.8˚N
22.6˚N
22.4˚N
western Changyun sand ridge
eastern Changyun sand ridge
subaqueous delta
40m
20m
10m
Taiwan Strait
Penghu Islands
Penghu Channel
subaqueous delta
Chiayi
Tainan
Kaohsiung
-50
-100
-150
-200

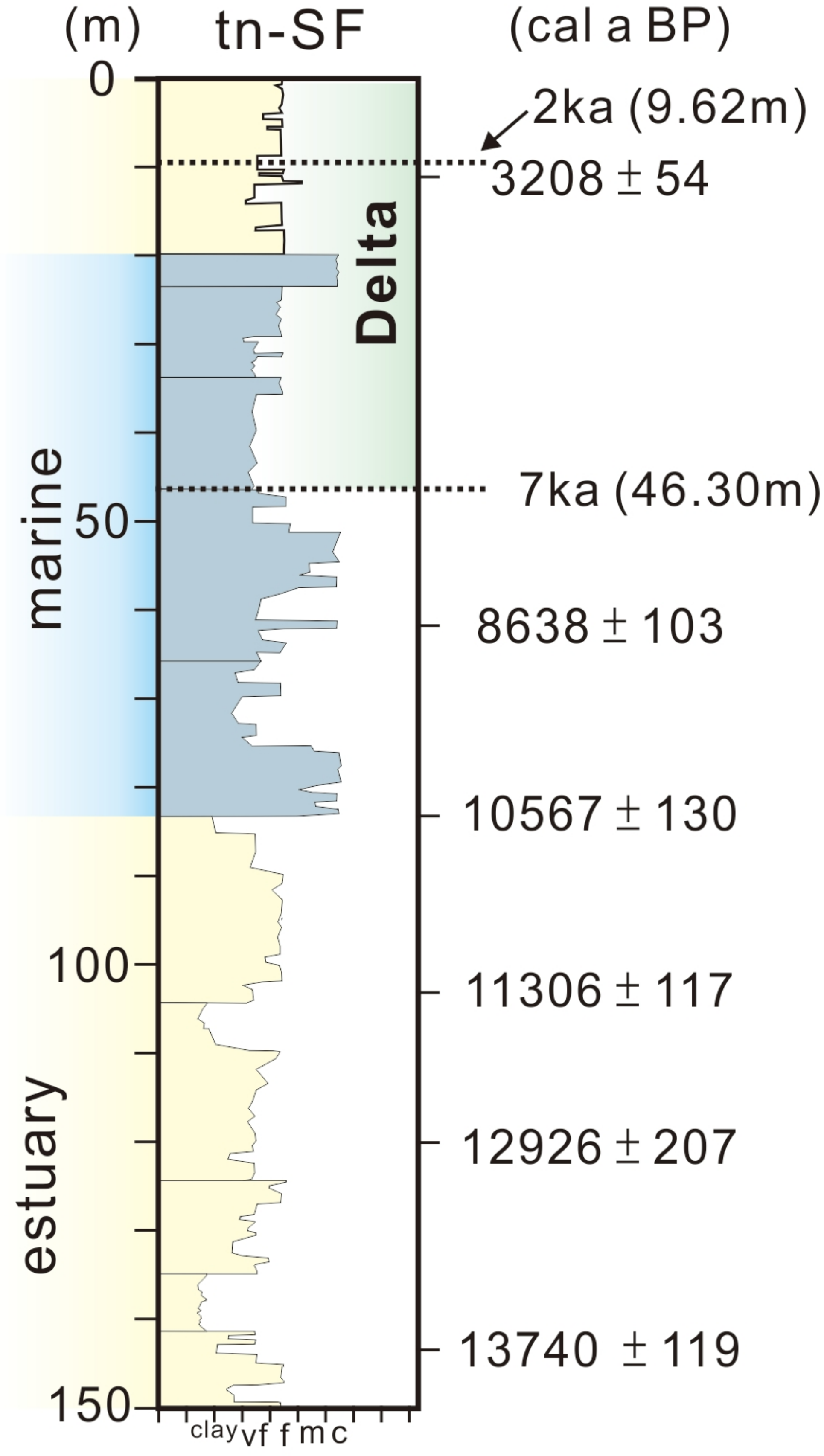

(m)
tn-SF
(cal a BP)
0
2ka (9.62m)
3208 ± 54
Delta
marine
50
7ka (46.30m)
8638 ± 103
10567 ± 130
100
11306 ± 117
estuary
12926 ± 207
13740 ± 119
150
clay
vf
f
m
c

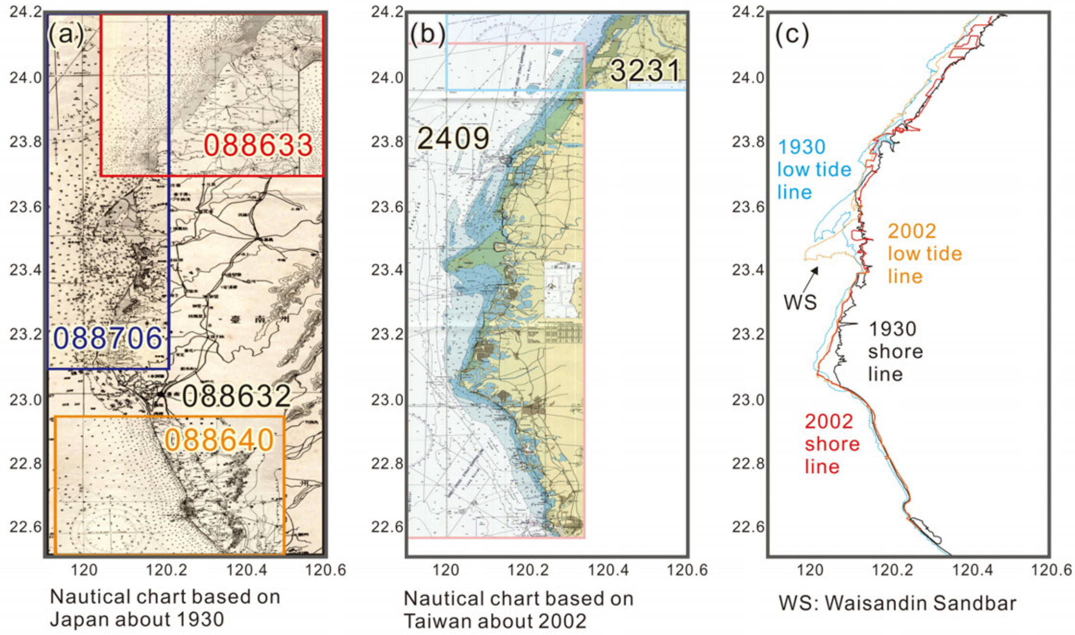

(a)
088633
088706
088632
088640
Nautical chart based on Japan about 1930
(b)
3231
2409
Nautical chart based on Taiwan about 2002
(c)
1930 low tide line
2002 low tide line
WS
1930 shore line
2002 shore line
WS: Waisandin Sandbar
24.2
24.0
23.8
23.6
23.4
23.2
23.0
22.8
22.6
120
120.2
120.4
120.6

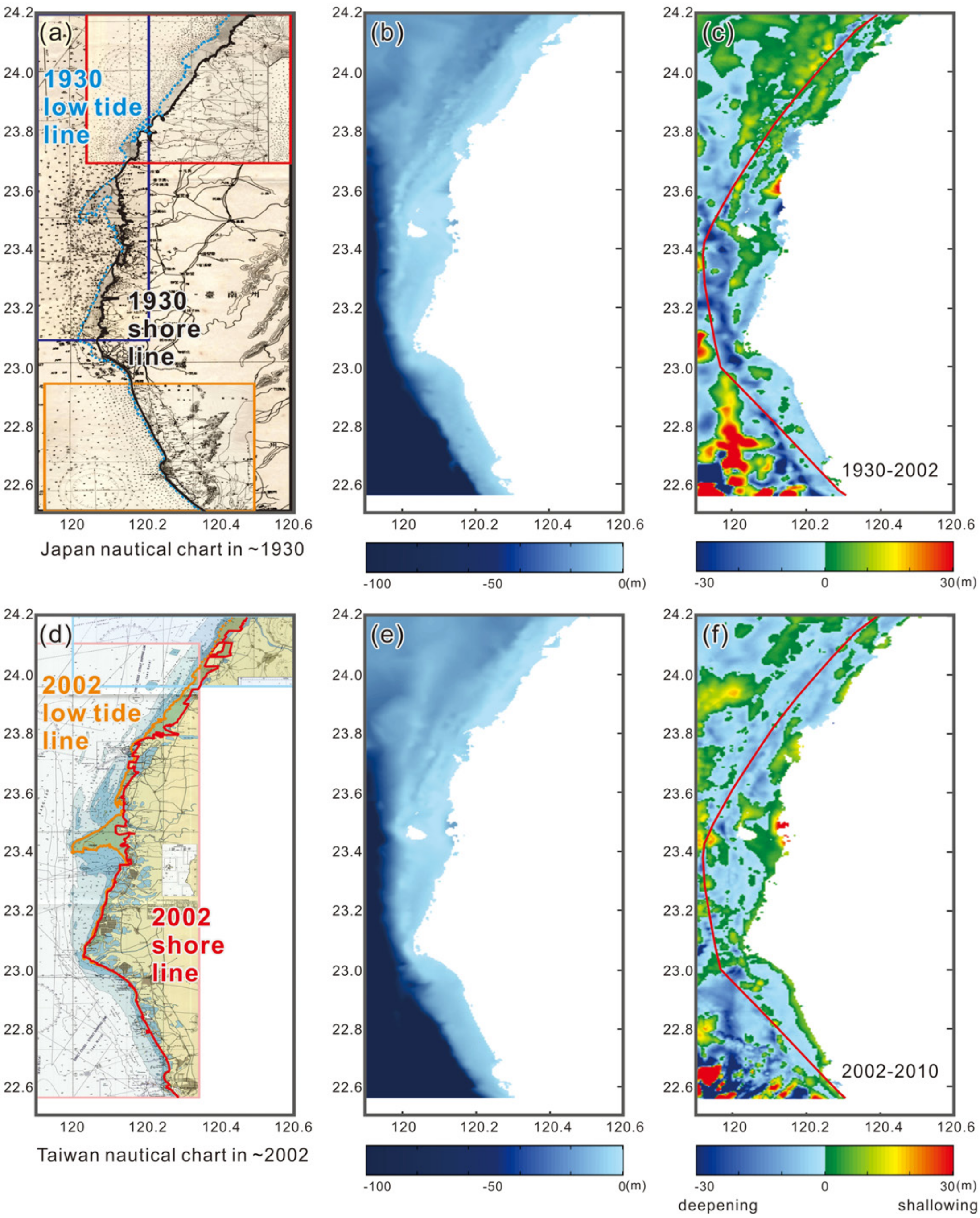

(a)
1930 low tide line
1930 shore line
Japan nautical chart in ~1930
(b)
(c)
1930-2002
-100
-50
0(m)
-30
0
30(m)
(d)
2002 low tide line
2002 shore line
Taiwan nautical chart in ~2002
(e)
(f)
2002-2010
deepening
shallowing
24.2
24.0
23.8
23.6
23.4
23.2
23.0
22.8
22.6
120
120.2
120.4
120.6

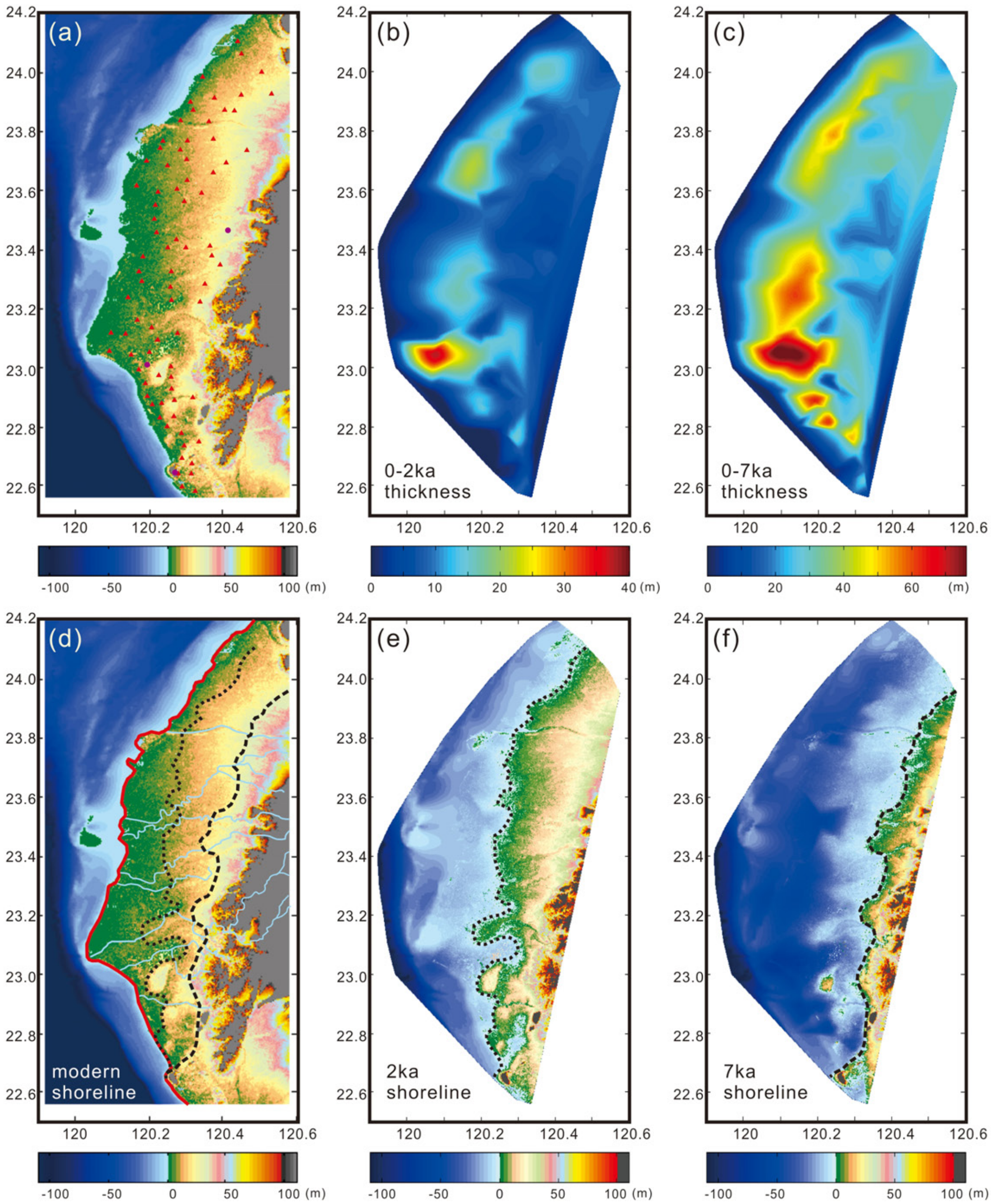

(a)
(b)
0-2ka
thickness
(c)
0-7ka
thickness
(d)
modern
shoreline
(e)
2ka
shoreline
(f)
7ka
shoreline
24.2
24.0
23.8
23.6
23.4
23.2
23.0
22.8
22.6
120
120.2
120.4
120.6
-100
-50
0
50
100 (m)
0
10
20
30
40 (m)
0
20
40
60
(m)

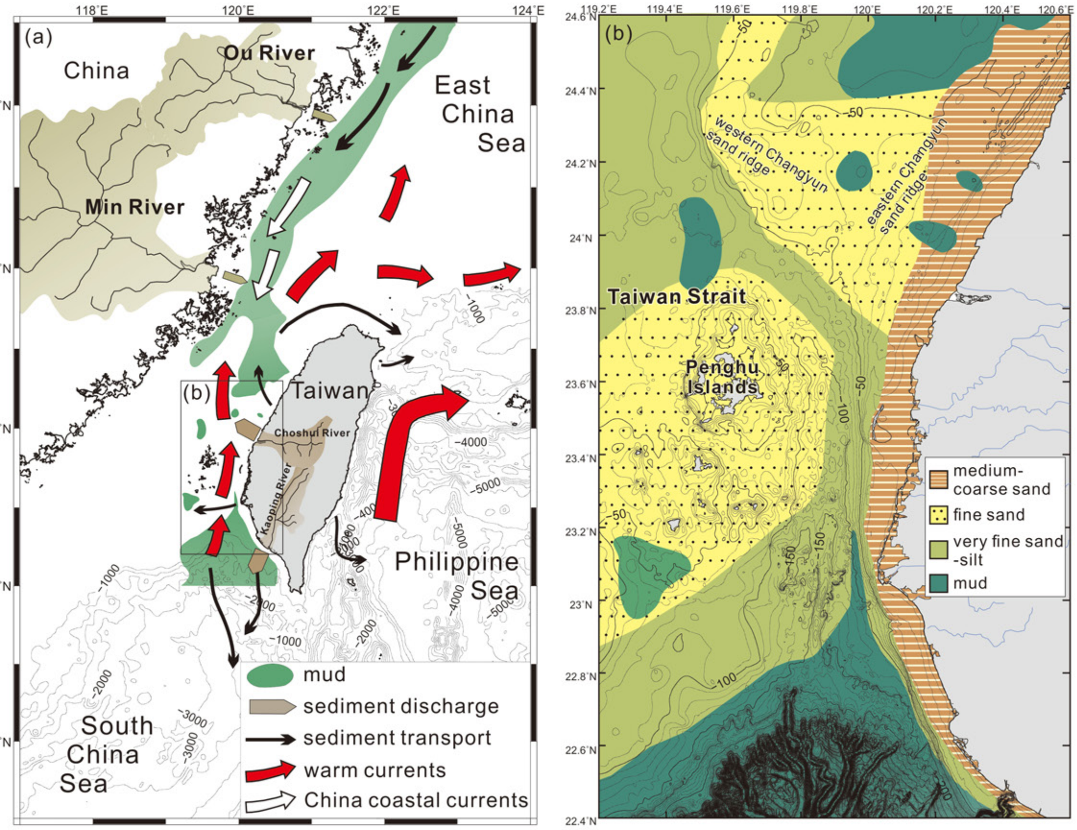

(a)
China
Ou River
East China Sea
Min River
Taiwan
Choshui River
Kaoping River
Philippine Sea
South China Sea
mud
sediment discharge
sediment transport
warm currents
China coastal currents
(b)
Taiwan Strait
Penghu Islands
western Changyun sand ridge
eastern Changyun sand ridge
medium-coarse sand
fine sand
very fine sand -silt
mud

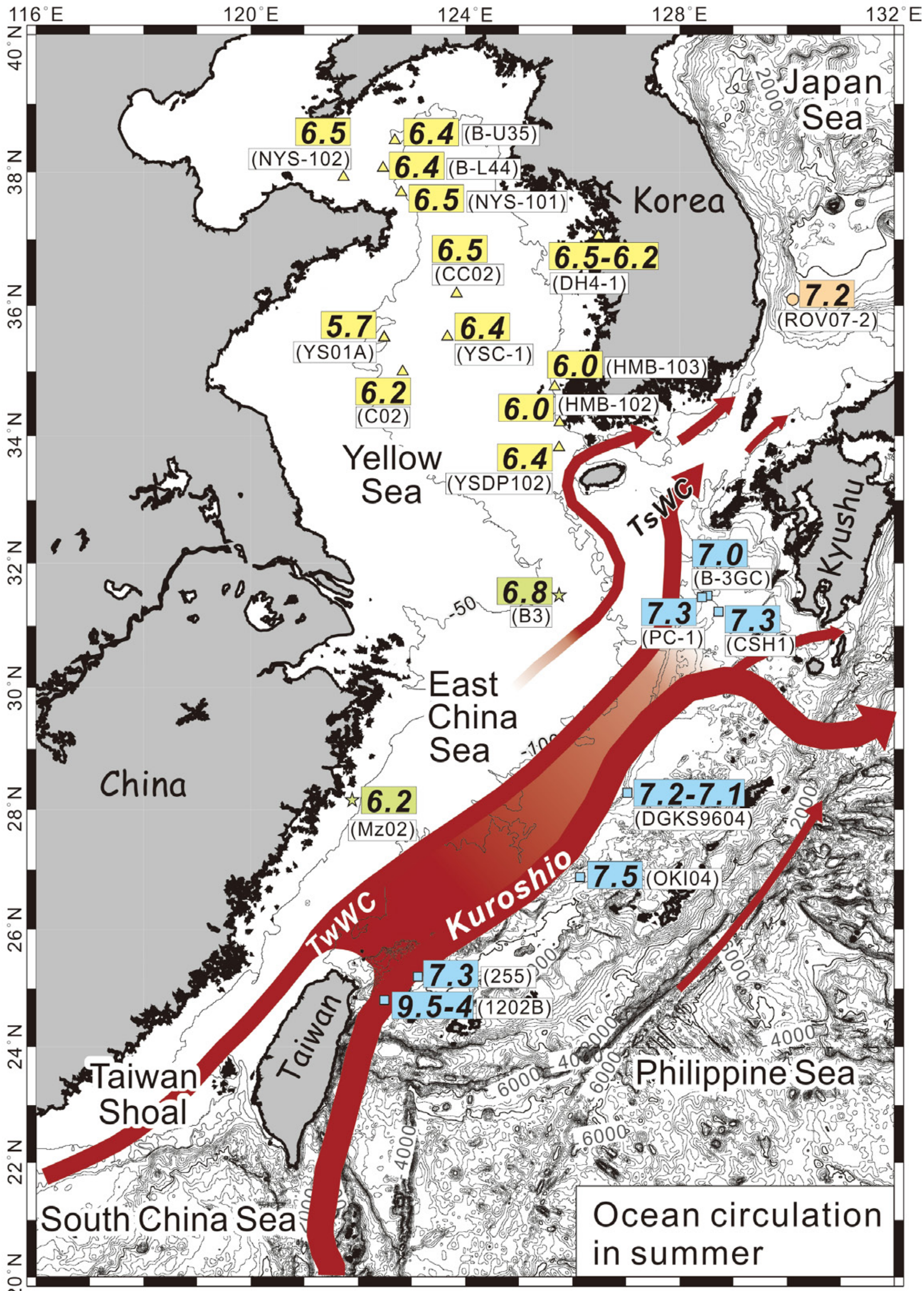

Japan Sea
Korea
Yellow Sea
East China Sea
China
Kyushu
Taiwan
Taiwan Shoal
South China Sea
Philippine Sea
TsWC
TwWC
Kuroshio
Ocean circulation in summer
6.5 (NYS-102)
6.4 (B-U35)
6.4 (B-L44)
6.5 (NYS-101)
6.5 (CC02)
6.5-6.2 (DH4-1)
7.2 (ROV07-2)
5.7 (YS01A)
6.4 (YSC-1)
6.0 (HMB-103)
6.2 (C02)
6.0 (HMB-102)
6.4 (YSDP102)
7.0 (B-3GC)
6.8 (B3)
7.3 (PC-1)
7.3 (CSH1)
6.2 (Mz02)
7.2-7.1 (DGKS9604)
7.5 (OKI04)
7.3 (255)
9.5-4 (1202B)
116°E
120°E
124°E
128°E
132°E
40°N
38°N
36°N
34°N
32°N
30°N
28°N
26°N
24°N
22°N
20°N

Table 1 Summary of the eight small mountainous rivers in the west and southwest Taiwan.

River name	Choshui	Peikang	Potzu	Pachang	Chishui	Tsengwen	Yenshui	Erhjen	**Total**
Drainage basin area (km^2)	3157	645	427	475	379	1177	343	350	6953
River length (km)	186.6	82.0	75.9	80.9	65.0	138.5	41.3	63.2	
Gradient in average	1/190	1/59	1/53	1/42	1/118	1/200	1/295	1/786	
Reservoir and dam	8	0	1	3	2	5	2	1	
Max elevation (m)	3400	520	1400	1900	550	2400	140	460	
Water discharge (km^3/y) Milliman & Farnsworth 2011	6.1	1	0.55	0.74	0.52	2.4	0.3	0.5	12.11
Sediment discharge (Mt/y)									
Milliman & Farnsworth, 2011	38	1.4	0.83	2.5	2.1	12	2.2	10	
Kao & Milliman, 2008	40 ± 5.7	1.4 ± 0.3	-	2.5 ± 0.5	-	12 ± 2.4	10 ± 2.1	-	
Lin et al., 2008	93.81	-	-	-	-	17.37	-	15.53	
Dadson et al., 2003	54	2	-	6	-	25	-	30	
Sediment discharge ranges	34.3 – 93.81	1.1- 2	0.83	2 - 6	2.1	9.6 - 25	2.2 – 12.1	10 - 30	62.1 – 171.84

References: Water Resources Agency, MOEA, Taiwan, ROC; Milliman & Farnsworth, 2011; Kao & Milliman, 2008; Lin et al., 2008; Dadson et al., 2003.

Table 2 Radiocarbon data in the Southwest Taiwan Delta.

Core ID	Sample Depth	^{14}C ages (a BP)	Calibrated age a BP (2 sigma)	Material	Reference
CH-SS	20.4	4410 ± 100	5184 - 5272	wood	Chen, 2010
CH-SS	49.8	13680 ± 170	16257 - 16781	wood	
CH-DF	34.95	7980 ± 50	8299 - 8394	shell	
CH-HB	19.2	1730 ± 80	2795 - 2629	shell	
CH-HB	46.6	7250 ± 110	7971 - 8174	wood	
CH-HT	19.2	12700 ± 80	14994 - 15265	wood	
CH-FY	27.6	3990 ± 70	4401 - 4570	wood	
CH-FY	42.5	6259 ± 86	6483 - 6689	shell	
CH JJ	80.0	3370 ± 80	3549 - 3700	wood	
CH JJ	280.0	22500 ± 280	26476 - 27147	wood	
CH-SH	33.1	7820 ± 90	8738 - 8752	wood	
CH-YL	33.2	6670 ± 70	7482 - 7592	wood	
CH-LS	64.2	12500 ± 80	14490 - 14989	wood	
CH-YD	37.8	7200 ± 100	7484 - 7663	shell	
CH-HH	38.6	8900 ± 70	10111 - 10173	organic mud	
CH-SG	41.5	6140 ± 70	6377 - 6549	shell	
CH-YA	35.8	8440 ± 60	9432 - 9524	organic mud	
CH-HA	23.4	2930 ± 70	2971 - 3171	wood	
CH-HA	31.0	4170 ± 65	3999 - 4203	shell	
CH-FR	14.5	5500 ± 70	5696 - 5864	shell	
CH-GH	27.1	6510 ± 40	7416 - 7476	organic carbon	
CH-SU	51.0	9610 ± 200	10686 - 11212	wood	
CY-GT	43.8	9410 ± 60	10571 - 10713	wood	Wu, 2007
CY-MDH	50.2	10340 ± 160	12478 - 12521	organic mud	
CY-NJ	9.6	4622 ± 57	5164 - 5281	organic mud	
CY-NJ	38.9	9517 ± 67	10953 - 11071	wood	
CY-SM	61.2	9880 ± 40	11235 - 11308	plant	
CY-LT	16.5	5070 ± 40	5368 - 5389	shell	
CY-LT	29.7	8490 ± 40	9485 - 9528	wood	
CY-BD	20.8	4360 ± 40	4867 - 4963	wood	
CY-BD	66.6	11800 ± 40	13659 - 13710	organic mud	
CY-BH	25.5	7250 ± 100	7982 - 8168	organic mud	
CY-AN	36.8	8180 ± 250	8326 - 8924	shell	
CY-TS	26.35	7277 ± 66	8028 - 8162	wood	
CY-SS	21.0	6653 ± 56	6998 - 7146	shell	
CY-SY	32.7	7415 ± 162	8152 - 8379	wood	
CY-LJ	21.2	7770 ± 40	8062 - 8175	shell	
CY-JH	31.5	5145 ± 57	5316 - 5452	shell	
CY-JH	86.3	9806 ± 57	11190 - 11253	wood	
CY-WS	30.3	4452 ± 59	4406 - 4566	shell	
CY-WS	70.7	9030 ± 57	9513 - 9649	shell	
CY-SW	17.3	2620 ± 80	2099 - 2296	shell	
CY-YA	35.8	8420 ± 60	9407 - 9520	organic mud	
TN-SK	44.7	7780 ± 40	8068 - 8186	shell	Lu, 2006
TN-AC	78.4	8970 ± 60	9458 - 9575	shell	

TN-GX	44.7	2822 ± 56	2332 - 2505	shell
TN-GX	91.45	9661 ± 71	10321 - 10524	shell
TN-TN	34.5	3150 ± 40	2758 - 2852	shell
TN-TN	129.5	11190 ± 80	12556 - 12681	shell
TN-YG	51.4	5359 ± 62	6240 - 6272	wood
TN-XG	21.2	6956 ± 77	7293 - 7434	shell
TN-DW	40.4	6355 ± 66	6625 - 6787	shell
TN-SG	35.6	4001 ± 56	3803 - 3965	shell
TN-SG	118.4	11957 ± 63	13257 - 13389	shell
TN-SF	11.1	1240 ± 62	3261 - 3154	shell
TN-SF	61.5	8253 ± 67	8535 - 8740	shell
TN-NK	18.85	2440 ± 60	2635 - 2696	wood
TN-NK	34.8	7850 ± 60	8159 - 8295	shell
TN-NH	75.3	9375 ± 59	10021 - 10191	shell
TN-ZD	34.6	8350 ± 60	8673 - 8897	shell
TN-ZH	12.5	8050 ± 70	8341 - 8483	shell
TN-YZ	22.3	7350 ± 40	7660 - 7757	shell
TN-CH	31.8	7220 ± 60	7545 - 7654	shell
TN-YC	9.65	6000 ± 60	6775 - 6911	wood
TN-SL	8.15	6570 ± 60	6879 - 7055	shell
TN-NZ	22.3	5360 ± 60	5568 - 5688	shell
TN-NZ	45.1	9920 ± 60	10642 - 10837	shell
TN-CC	38.4	37420 ± 480	41503 - 42200	wood
TN-WC	9.7	5800 ± 60	6020 - 6181	shell
TN-XG	6.7	6070 ± 70	6298 - 6446	shell
TN-DS	1.62	6250 ± 60	7156 - 7260	wood
TN-GS	16.69	5330 ± 60	5524 - 5656	shell
TN-GS	55.29	9690 ± 70	10367 - 10563	shell
TN-WL	45.55	5410 ± 60	6181 - 6291	wood
TN-AL	25.01	5970 ± 60	6218 - 6347	shell
TN-YJ	8.67	6160 ± 40	6417 - 6530	shell
TN-JH	50.7	8780 ± 40	9839 - 9888	wood
TN-CG	29.4	4440 ± 60	4397 - 4559	shell
TN-CG	105.1	8940 ± 60	10121 - 10197	wood
TN-YH	6.8	1760 ± 40	2287 - 2183	wood
TN-YH	103.1	9420 ± 50	10586 - 10704	wood
TN-MT	4.8	4640 ± 60	4672 - 4823	shell
TN-MT	30.4	6540 ± 60	6837 - 7007	shell
TN-CJ	14.5	3420 ± 60	3067 - 3247	shell
TN-CJ	18.19	6470 ± 130	7264 - 7494	organic mud
TN-XD	20.6	3300 ± 60	2908 - 3102	shell
TN-XD	27.2	4480 ± 40	5164 - 5282	wood

Table 3 The total volumes and partial volumes above/below modern sea level of the Southwest Taiwan Delta (SWTD)

cal ka BP age interval	Total Volume (km^3)	Weight (Mt/y)	Volume above sea level (km^3)	Volume above sea level Percentage (%)	Volume below sea level (km^3)	Volume below sea level Percentage (%)
0–7	201.72	46.11	46.03	22.8	155.69	77.2
0–1	29.81	47.69	7.87	26.4	21.94	73.6
1–2	30.33	48.54	6.61	21.8	23.73	78.2
2–3	26.46	42.33	5.48	20.7	20.98	79.3
3–4	26.47	42.35	5.54	20.9	20.93	79.1
4–5	26.73	42.76	5.77	21.6	20.96	78.4
5–6	27.94	44.71	6.18	22.1	21.76	77.9
6–7	33.98	54.37	8.58	25.2	25.40	74.8
average/ka	28.82	46.11	6.58	22.8	22.24	77.2